land

MDPI

Article

Remote Sensing Identification of Major Crops and Trade-Off of Water and Land Utilization of Oasis in Altay Prefecture

Gaowei Yan [1,2], Luguang Jiang [1,2,*] and Ye Liu [1]

[1] Institute of Geographic Sciences and Natural Resources Research, Chinese Academy of Sciences, Beijing 100101, China
[2] College of Resources and Environment, University of Chinese Academy of Sciences, Beijing 100049, China
* Correspondence: jianglg@igsnrr.ac.cn

Abstract

The Altay oasis, located at the heart of the transnational ecological conservation zone shared by China, Kazakhstan, Russia, and Mongolia, is a region with tremendous potential for water resource utilization. However, with the continued expansion of agriculture, its ecological vulnerability has become increasingly pronounced. Within this fragile balance lies a critical opportunity: efficient water resource management could pave the way for sustainable development across the entire arid oasis regions. This study uses a decision tree model based on a feature threshold to map the spatial distribution of major crops in the Altay Prefecture oasis, assess their water requirements, and identify the coupling relationships between agricultural water and land resources. Furthermore, it proposed optimization planting structure strategies under three scenarios: water-saving irrigation, cash crop orientation, and forage crop orientation. In 2023, the total planting area of major crops in Altay Prefecture was 3368 km^2, including spring wheat, spring maize, sunflower, and alfalfa, which consumed 2.68 $\times$ 10^9 m^3 of water. Although this area accounted for only 2.85% of the land, it consumed 26.23% of regional water resources, with agricultural water use comprising as much as 82.5% of total consumption, highlighting inefficient agricultural water use as a critical barrier to sustainable agricultural development. Micro-irrigation technologies demonstrate significant water-saving potential. The adoption of such technologies could reduce water consumption by 14.5%, thereby significantly enhancing agricultural water-use efficiency. Cropping structure optimization analysis indicates that sunflower-based planting patterns offer notable water-saving benefits. Increasing the area of sunflower cultivation by one unit can unlock a water-saving potential of 25.91%. Forage crop combinations excluding soybean can increase livestock production by 30.2% under the same level of water consumption, demonstrating their superior effectiveness for livestock system expansion. This study provides valuable insights for achieving sustainable agricultural development in arid regions under different development scenarios.

Keywords: crop identification; Sentinel-2; water and land balance; scenario simulation; Altay Prefecture

check for updates

Academic Editor: Mateus Batistella

Received: 10 June 2025
Revised: 29 June 2025
Accepted: 5 July 2025
Published: 7 July 2025

Citation: Yan, G.; Jiang, L.; Liu, Y. Remote Sensing Identification of Major Crops and Trade-Off of Water and Land Utilization of Oasis in Altay Prefecture. *Land* **2025**, *14*, 1426. https://doi.org/10.3390/land14071426

Copyright: © 2025 by the authors. Licensee MDPI, Basel, Switzerland. This article is an open access article distributed under the terms and conditions of the Creative Commons Attribution (CC BY) license (https://creativecommons.org/licenses/by/4.0/).

1. Introduction

Oasis ecosystems are complex regional ecological systems formed under the constraints of limited water resources and are indispensable in arid and semi-arid regions. They provide conditions suitable for stable vegetation growth and human habitation [1,2]. As a unique geographical, ecological, and economic complex system in arid regions [3],

oases are directly linked to regional food security, ecological balance, and socio-economic stability [4,5]. The ecological vulnerability and economic importance of oases in the arid regions of northwest China are in sharp contrast: less than 4% of the land area accommodates over 90% of the population and more than 95% of social wealth, and this has made oases in arid regions become key challenging areas for sustainable development [6,7].

Despite their critical importance, oases are confronted with multiple and interrelated crises, including notably escalating water scarcity [8], ecosystem degradation, and unsustainable agricultural practices [9–12]. Climate change projections exacerbate these challenges. According to the IPCC AR6, renewable water resources across arid regions of Central Asia are expected to decrease by 23–41% by 2050 [13]. Recent studies further highlight the growing water insecurity in Central Asia; the conflict between limited water availability and expanding agricultural land has already triggered cascading ecological and economic crises [14,15], as illustrated by the 2020 seasonal drying of the Tarim River, which forced the abandonment of 170,000 hectares of farmland [16]. Consequently, optimizing the allocation of water and land resources has emerged as a pivotal challenge for achieving sustainable oasis development.

In recent years, as research on oases has progressively deepened, scholars have increasingly acknowledged the central role of agricultural water use in shaping human–water interactions in arid regions [17–19]. Studies have shown that agricultural water use in the oasis regions of northwest China's arid zones represents more than 90% of total water consumption [20]. The expansion of cultivated land and the reliance on flood irrigation practices have significantly increased water demand, often exceeding local supply capacities. Unsustainable water-use patterns have not only contributed to groundwater depletion and salinization but also exacerbated land degradation and desertification processes [21–27]. Its precise quantification and efficient management have emerged as focal scientific challenges in ensuring the sustainable utilization of water resources in arid regions. However, although existing studies have primarily estimated and analyzed agricultural water resources in oases at the macro-scale, fine-scale investigations that uncover underlying patterns and system characteristics are still lacking in detail and depth [28–30], and this limitation has significantly hindered the achievement of the optimized allocation and efficient use of water resources [31].

The accurate extraction of crop structures and areas constitutes an essential foundation for the precise management of agricultural water resources [32]. Although large-scale studies have achieved significant advances in crop structure mapping, the complex agricultural patterns in oasis regions present challenges to the accurate extraction of crop structures at high resolution [33–35]. Traditional single-image spectral classification methods, such as Maximum Likelihood and Support Vector Machines, face significant limitations in crop identification due to the inherent spectral confusion during critical crop growth stages [36]. This challenge is particularly pronounced in oasis regions, characterized by complex and diverse cropping patterns, where the applicability of these methods is further diminished [37]. In contrast, time-series classification methods have demonstrably improved identification accuracy by leveraging phenological information throughout the crop growing season. However, much of the existing research in this area has relied on low-spatiotemporal-resolution imagery from platforms like MODIS and Landsat [38], which are insufficient for the high-precision crop identification required for the small land parcels typical of oasis environments. More recently, decision tree methods, integrating vegetation index time series with crop phenological features and expert knowledge, have shown promising small-sample adaptability and interpretability [39,40]. Despite these advancements, the effectiveness of such models is contingent on high-quality remote sensing data, and the

regional variability of crop phenological characteristics presents a considerable challenge to their broader generalization and application [41,42].

In order to better achieve the efficient utilization and optimized allocation of agricultural water resources in arid regions, it is crucial to accurately understand crop water requirements [43–45]. Crop water demand is typically estimated based on reference crop evapotranspiration and crop coefficients. As the standard approach recommended by the Food and Agriculture Organization (FAO) of the United Nations, the Penman-Monteith model offers a more accurate estimation of reference evapotranspiration compared to that of empirical formulas [46,47]. Crop coefficients characterize the water requirements of crops at different growth stages [48]. Therefore, by accurately calculating reference evapotranspiration using the Penman-Monteith equation and integrating crop coefficients for crop phenology in oasis regions, a water demand estimation model grounded in crop physiological characteristics can be established [49]. This approach not only provides a robust theoretical and technical foundation for the sustainable development of oasis agriculture in water-scarce arid regions but also lays a scientific basis for the optimized allocation and efficient utilization of regional water resources.

Oasis agriculture faces an urgent need to balance crop structure optimization with efficient water resource utilization due to increasingly severe water scarcity. Existing research has attempted to use multi-objective optimization models (e.g., linear programming, fuzzy optimization, genetic algorithms) to simulate water and land resource allocation strategies under different crop combinations [50–52]. These efforts have, to some extent, achieved regional crop layout optimization and improved resource-use efficiency. However, current research still has three main shortcomings: A comprehensive and systematic evaluation framework for the coupling mechanisms among water, soil, and crops has yet to be established. Most optimization models depend on static data, making it difficult to reflect dynamic uncertainties such as climate change and market fluctuations. Existing methods are often constrained by variations in natural geography and socioeconomic conditions, hindering their replicability and broad applicability across different regions [53–55].

While existing research has provided valuable insights into oasis agriculture and water management, many studies have focused on well-known oasis systems such as those in the Tarim or Hexi regions, resulting in knowledge gaps regarding other critical regions [3,56–62]. Altay Prefecture in northern Xinjiang is one such overlooked but crucial region. Altay Prefecture, as a transition zone between arid and semi-arid ecosystems, hosts unique oasis systems where rapid agricultural expansion has led to a sharp increase in water demand. This makes Altay not only a representative site for studying the intricacies of oasis agricultural water use but also a frontier region for testing innovative water and land optimization strategies. Its geographic setting and socio-economic transformation offer a unique lens for examining sustainable oasis development in a broader Central Asian context.

In light of this, the present study focuses on the coupling relationship between agricultural land and water resources in the oasis region of Altay Prefecture. By leveraging remote sensing technology, we accurately extract the complex crop structure and spatial distribution within the oasis. Combined with meteorological data, a crop water requirement model based on crop physiological characteristics is constructed to reveal the water resource response mechanisms under multiple cropping structures in multiple scenarios. The findings provide a scientific basis and decision-making support for the efficient management and sustainable development of land and water resources in Altay and wider arid-zone oases.

2. Materials and Methods

2.1. Study Area

Altay Prefecture (45°00′–49°10′ N, 85°31′–91°04′ E) is located at the junction of China, Kazakhstan, Russia, and Mongolia, situated on the southwestern slope of the central Altay Mountains and the northern edge of the Junggar Basin. Covering a substantial area of 1.18×10^5 km^2, the prefecture accounts for approximately 7.1% of Xinjiang's total landmass in China. Administratively, it comprises six counties and two cities, namely Altay City, Beitun City, Burqin County, Habahe County, Jeminay County, Fuhai County, Fuyun County, and Qinghe County (Figure 1). The area experiences a temperate continental cold climate, characterized by low precipitation, high evaporation, and ample sunlight. The average annual precipitation ranges from 131 to 223 mm, while the annual evaporation rate is between 1367 and 2066 mm. The annual average total water resources in Altay Prefecture are 10.18×10^9 m^3, making it one of the water-rich areas in Xinjiang, China. Its hydrology is dominated by three major river systems: the Irtysh River and the Ulungur River, both originating from the Altai Mountains, and the Jeminay Mountain Stream, which originates from the Saur Mountains. These three river systems collectively drain an area of 9.57×10^4 km^2.

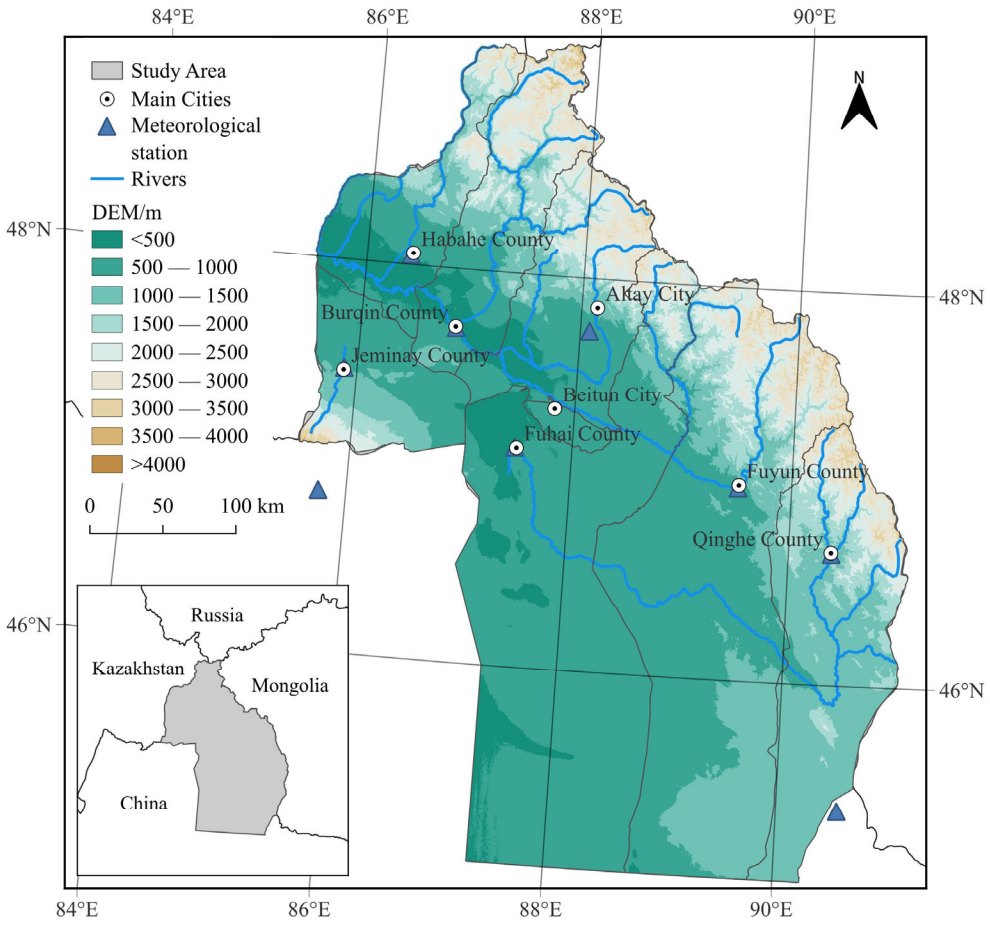

Figure 1. Location and elevation of Altay Prefecture.

The vegetation cover in Altay Prefecture exhibits a clear vertical zonation pattern. Forests and alpine meadows dominate the mountainous areas, while the plain regions are largely characterized by arid desert landscapes with sparse vegetation, including extensive bare soil and Gobi surfaces. These areas are marked by low precipitation and high evaporation rates. Oases, vital for agricultural activity, are primarily distributed across

the alluvial plains of these river valleys. In the plains, the soil-type transition from north to south, consisting of brown calcic soil, light brown calcic soil, gray-brown desert soil, and eolian sandy soil. These soils commonly share characteristics such as being thin-layered, coarse-textured, high in gravel content, and highly permeable. While this soil structure aids in both precipitation infiltration and groundwater recharge, its poor water-holding capacity makes it susceptible to significant water loss through evapotranspiration.

Agricultural practices in Altay Prefecture primarily involve a one-year ripening system. This includes spring wheat, spring maize (comprising both grain maize and silage maize varieties), and sunflower (categorized into edible and oilseed types). Additionally, alfalfa is harvested multiple times annually. Currently, agricultural irrigation predominantly relies on traditional flood irrigation methods. This approach results in a notably low irrigation efficiency, with a water-use efficiency coefficient for agriculture estimated at only 0.55. The livestock sector in the region largely centers on beef cattle breeding, with their primary feed sources being silage corn, forage, grain corn, and soybeans.

2.2. Materials

This study utilized Sentinel-2 Level-2A imagery with a spatial resolution of 10 m, accessed via the Google Earth Engine (GEE) platform. Sentinel-2 imagery includes three quality assessment (QA) bands, among which QA60 contains cloud mask information. Cloud removal was performed using threshold-based filtering of the QA60 band and other cloud masking techniques available in the GEE. Based on cloud-free imagery, land-cover interpretation keys were established.

Sample data were meticulously collected through field surveys conducted by our research team in the Altay region during August 2023 and July 2024. We acquired a total of 390 samples, distributed as follows: 100 for spring wheat, 100 for spring maize, 30 for sunflower, 80 for alfalfa, 30 for forestland, and 50 for grassland. The sample design strategically considered the relatively concentrated crop planting structure and the distinct phenological differences among crops within the study area. A decision tree model was selected for classification due to its robustness with small sample sizes, making it particularly well suited for classification tasks with limited available samples. Furthermore, to effectively mitigate the impact of insufficient minority class samples on classification performance, we integrated vegetation index time-series curves with expert knowledge to define phenological thresholds. This study employed daily meteorological data averaged over 44 years (1980–2023) from ten meteorological stations in and around Altay Prefecture, including precipitation, maximum temperature, minimum temperature, average temperature, vapor pressure, average wind speed, net radiation, and other data. These data were obtained from the China Meteorological Data Service Center (https://data.cma.cn, accessed on 13 August 2023).

Watershed boundary vector data were extracted through hydrological analysis in ArcGIS, utilizing the SRTM 30 m Digital Elevation Model (DEM) acquired from the Google Earth Engine (GEE) platform [63,64]. Water resource data were acquired from the *Xinjiang Uygur Autonomous Region Water Resources Bulletin* and the *Hydrological Yearbook of the People's Republic of China-Irtysh River Basin Hydrological Data*. Statistical data such as population size and crop cultivated area were sourced from the *Altay Prefecture Statistical Yearbook*.

2.3. Methods

2.3.1. Research Framework

This research framework consists of three main components: first, extracting the spatial distribution of major crops using Sentinel-2 remote sensing data and a decision tree model; second, calculating crop water requirements and irrigation needs based on

the Penman-Monteith model; and finally, analyzing different land and water resource allocation scenarios through multi-scenario simulations to assess the trade-offs between crop cultivation and water resource use, providing support for the optimized management of agricultural water resources (Figure 2).

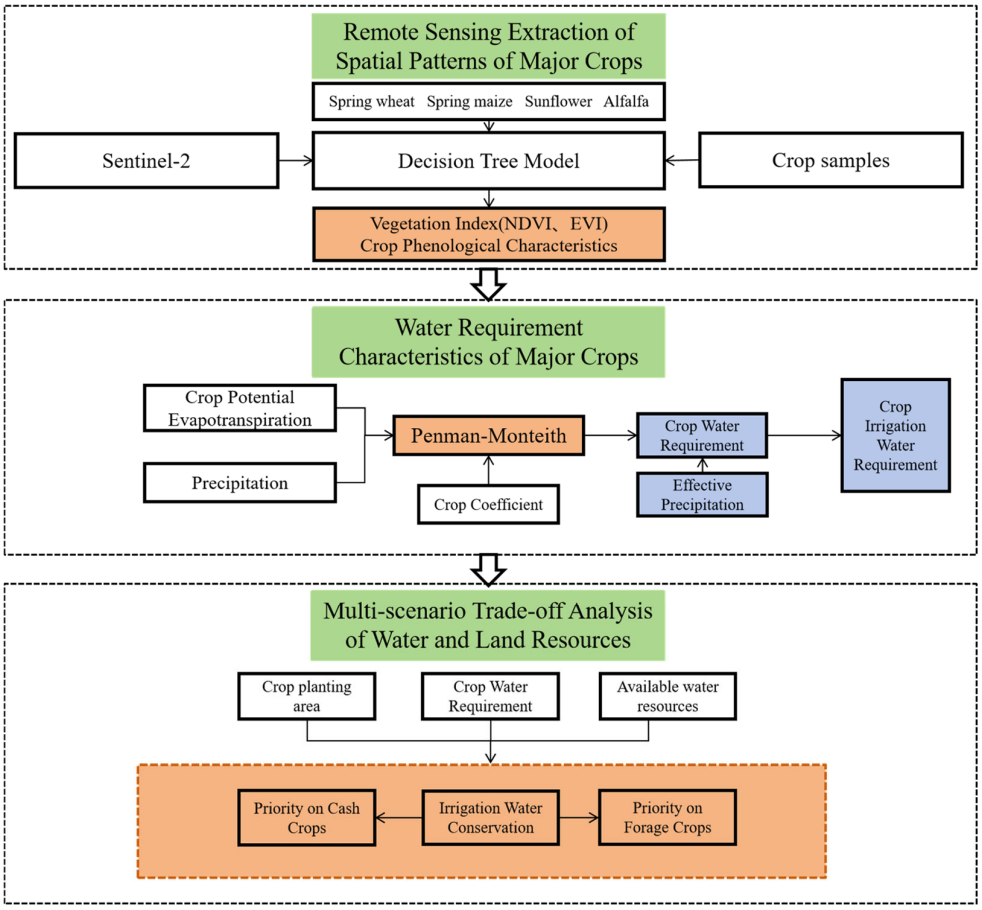

Figure 2. The research framework.

2.3.2. Remote Sensing Extraction of Crops

This study focuses on the 2023 calendar year. This specific timeframe was chosen primarily because it aligns directly with the sample data collected during our field expeditions in 2023–2024 and the latest official crop statistical data released for the Altay region. This ensures both the reliability and timeliness of our crop remote sensing image interpretation and classification. Furthermore, this synchronicity facilitates the cross-validation of our remote sensing extraction results. For the purpose of extracting crop phenological features and developing classification models, we utilized the GEE platform to synthesize the NDVI (Normalized Difference Vegetation Index) and EVI (Enhanced Vegetation Index) time-series data from Sentinel-2 imagery, covering the full year from January to December 2023. The Normalized Difference Vegetation Index (NDVI) is a widely used remote sensing metric, calculated as the ratio of the difference between near-infrared (NIR) and red (R) reflectance to their sum. It is a foundational tool for vegetation monitoring, crop identification, and land-cover classification [65–67]. The Enhanced Vegetation Index (EVI) offers a more refined measure, exhibiting greater sensitivity to changes in the vegetation canopy structure, including the Leaf Area Index (LAI) and canopy type. The EVI incorporates atmospheric correction factors and soil adjustment parameters to effectively reduce interference from atmospheric scattering and soil background noise. This also helps mitigate the saturation issue that the NDVI can experience in areas with high vegetation cover, allowing the EVI to

more accurately reflect the true physiological status of vegetation [68,69]. The formula is as follows:

$$NDVI = \frac{NIR - R}{NIR + R} \quad (1)$$

$$EVI = G \times \frac{NIR - R}{NIR + C_1 \times R - C_2 \times BLUE + L} \quad (2)$$

In the formula, *NIR* and *R* represent the reflectance values of the near-infrared and red spectral bands, respectively. *G* is a gain factor, typically set to 2.5. C_1 and C_2 are adjustment factors used to correct for atmospheric scattering effects in the red and blue bands, with commonly used values of 6 and 7.5, respectively. *BLUE* denotes the reflectance value of the blue band. *L* is a constant used for atmospheric scattering correction, typically assigned a value of 1.

Raw vegetation index time-series data often contain anomalies and noise due to factors like cloud cover and aerosols in remote sensing imagery. To address this, we used the Savitzky–Golay (S-G) filtering method to smooth the time-series data. A 7-day time window was applied during this smoothing process. This approach helps preserve critical crop phenological features while simultaneously enhancing data continuity and stability [70].

Major agricultural crops exhibit distinct growth rhythms, which are clearly reflected as varying phenological features in their vegetation index time-series data. By analyzing the characteristic changes in the NDVI and EVI time-series curves for key crops, we can extract critical phenological nodes. These nodes serve as crucial discriminators for differentiating among various crop types. Building on this, we developed a decision tree classification rule set that leverages these phenological features and vegetation index thresholds. This approach allows for the fine-grained identification of spring wheat, spring maize, sunflower, and alfalfa.

As shown in Figure 3, spring wheat is the earliest sown crop in the Altay region, reaching its NDVI peak in early June. It can be identified as spring wheat if the NDVI value exceeds 0.13 during the period from Day of Year (DOY) 156 to 163. Spring maize reaches its maximum NDVI between mid-July and early August and is classified within the spring maize planting area when the NDVI exceeds 0.19 during DOY 196 to 216. Sunflower enters the EVI saturation phase from late June to mid-July and is identified as sunflower if the EVI value is greater than or equal to 0.9 between DOY 176 and 198. Alfalfa exhibits multiple EVI peaks and troughs throughout its growth cycle. Two identification strategies are employed to account for different harvest cycles of alfalfa: (1) The first type is characterized by EVI > 0.7 during DOY 156–163, EVI < 0.5 during DOY 186–206, and EVI > 0.7 during DOY 226–236. (2) The second type satisfies EVI > 0.7 during DOY 205–219, EVI < 0.57 during DOY 226–240, and EVI > 0.64 during DOY 247–268.

To comprehensively evaluate the crop classification results derived from the decision tree algorithm, this study employed a confusion matrix for quantitative accuracy assessment. Validation samples were obtained through a combination of field surveys and high-resolution remote sensing image interpretation. Based on the constructed confusion matrix, we calculated the overall accuracy, Kappa coefficient, User accuracy, and producer accuracy. The classification achieved an overall accuracy exceeding 93% and a Kappa coefficient greater than 0.9, indicating a high level of reliability in the classification results. Specifically, spring wheat and spring maize demonstrated high User accuracy and Producer accuracy due to their distinct phenological characteristics and ample sample sizes. Although sunflower and alfalfa had smaller sample sets, their identification was robust, benefiting from time-series threshold constraints and expert rule support (Table 1).

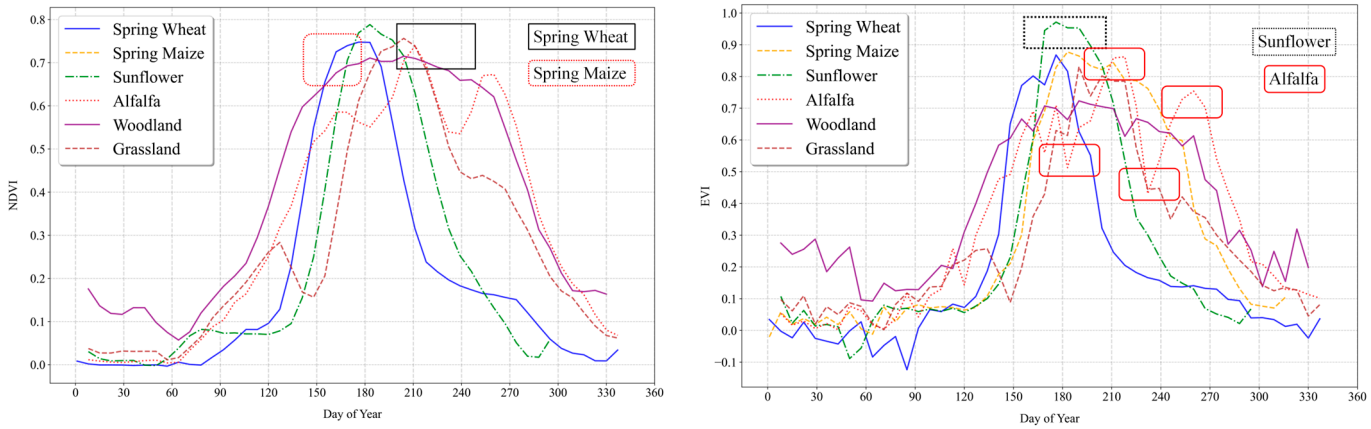

(**a**) (**b**)

Figure 3. Vegetation index change curves of major crops in Altay Prefecture. (**a**) NDVI time-series curves of major land-cover types. (**b**) EVI time-series curves of major land-cover types.

Table 1. Accuracy assessment of major crop classification.

	Spring Wheat	Spring Maize	Sunflower	Alfalfa
Overall Accuracy	93.08	-	-	-
Kappa	0.90	-	-	-
Producer's Accuracy	91.00	94.35	97.50	89.73
User's Accuracy	92.31	91.43	95.26	87.80

2.3.3. Crop Water Requirements

The crop coefficient method recommended by FAO-56 has been widely applied in studies of crop water requirements during different growth stages. This method, based on crop type and growth stage, enables the estimation of crop water requirements at various developmental stages [44]. The model parameters in the Penman-Monteith equation can be adjusted using field-measured crop coefficients and growth stage division. The formula is as follows:

$$W_{i,\mathrm{veg}} = ET_0 \times K_\mathrm{i} \tag{3}$$

In the formula, $W_{\mathrm{i,veg}}$ is the total water requirement of the i crop during its growth period; ET_0 is the reference crop evapotranspiration (mm); and K_i is the crop coefficient for the i crop.

Numerous experimental studies have demonstrated that the Penman-Monteith equation, recommended by the Food and Agriculture Organization (FAO) in 1998, can provide highly accurate estimates of reference crop evapotranspiration [45,71]. The formula is as follows:

$$ET_0 = \frac{0.408\Delta(R_\mathrm{n} - G) + \gamma\frac{900}{273+T}u_2(e_\mathrm{a} - e_\mathrm{d})}{\Delta + \gamma(1 + 0.34u_2)} \tag{4}$$

In the formula, ET_0 is the reference crop evapotranspiration (mm/day); Δ is the slope of the saturation vapor pressure–temperature curve (kPa/°C); R_n is the net radiation at the crop surface (MJ/m^2/day); G is the soil heat flux density (MJ/m^2/day); γ is the psychrometric constant (kPa/°C); T is the mean daily air temperature at 2 m height (°C); u_2 is the mean daily wind speed at 2 m height (m/s); and e_a and e_d are the saturation vapor pressure and actual vapor pressure (kPa).

The effective precipitation refers to the portion of precipitation that can be directly absorbed by crops for evapotranspiration, excluding surface runoff and deep percolation beyond the root zone that is unavailable for plant uptake. In this study, we employed the calculation method recommended by the Soil Conservation Service (SCS) of the United

States Department of Agriculture (USDA) to calculate effective precipitation [72]. The formula is as follows:

$$P_{i,eff} = \begin{cases} P \times \frac{4.17-0.2P}{4.17}, & P \leq 8.3 \text{ mm} \\ 4.17 + 0.1P, & P > 8.3 \text{ mm} \end{cases} \quad (5)$$

In the formula, $P_{i,eff}$ represents the daily effective precipitation (mm), and P denotes the daily total precipitation (mm).

The crop irrigation water requirement can be calculated as the difference between the total crop water requirement during the growth period and the effective precipitation [20]. The formula is as follows:

$$W_{i,irr} = W_{i,veg} - P_{i,eff} \quad (6)$$

In the formula, $W_{i,irr}$ represents the irrigation water requirement for crop i during its growth period; $W_{i,veg}$ denotes the total water requirement for crop i during its growth period; and $P_{i,eff}$ indicates the effective precipitation for crop i during its growth period. All values are expressed in millimeters (mm).

To enable the spatial visualization and quantitative analysis of crop water requirement indicators, we utilized the Inverse Distance Weighting (IDW) interpolation algorithm within the ArcGIS 10.8 platform. This method uses the discrete crop water requirement characteristics calculated from individual meteorological stations as sample data. Through IDW interpolation, a spatially continuous raster dataset was constructed, effectively transforming point-based observations into a comprehensive spatial representation of crop water demand across the study area.

This study leveraged field-observed crop phenology data collected during surveys to divide the complete crop growth cycle into four distinct stages. The Initial Growth Stage; The Rapid Development Stage; The Mid-Season Stage. The Late-Season Stage (maturity) (Table 2).

Table 2. Division of major crop growth stages.

Crop Type	Initial Stage	Rapid Development Stage	Mid-Season Stage	Late-Season Stage	Entire Growing Season
Spring Wheat	04.25–06.09	06.10–07.04	07.05–08.17	08.18–08.25	04.25–06.09
Spring Maize	05.15–07.04	07.05–08.01	08.02–09.04	09.05–09.20	05.15–07.04
Sunflower	05.15–07.14	07.15–08.04	08.05–08.14	08.15–09.15	05.15–07.14
Alfalfa (First Cut)	05.03–05.24	05.25–06.15	06.16–07.04	-	05.03–05.24
Alfalfa (Second Cut)	07.05–07.19	07.20–08.04	08.05–09.05	-	07.05–07.19

The crop coefficients (K_c) used in this research are based on findings from relevant studies conducted in the Altay region and northern Xinjiang [64,73–75]. For each growth stage, the daily average of crop coefficients within that period was used as the representative crop coefficient for that specific stage. Furthermore, the average of these stage-specific crop coefficients was adopted as the parameter for calculating the crop's total water requirement over its entire growing season (Table 3).

Table 3. Crop coefficient by growth stage for major crops.

Crop Type	Initial Stage	Rapid Development Stage	Mid-Season Stage	Late-Season Stage	Entire Growing Season
Spring Wheat	0.86	1.05	1.09	0.67	0.92
Spring Maize	0.8	0.96	1.03	0.79	0.90
Sunflower	0.64	1.04	1.12	0.64	0.85
Alfalfa (First Cut)	0.94	1.03	0.86	-	0.94
Alfalfa (Second Cut)	0.51	1.18	1.09	-	0.94

2.3.4. Multi-Scenario Trade-Off Analysis of Water and Land Resources

This study designs three distinct crop structure optimization scenarios, each with different development objectives, to simulate and analyze the complex interplay and trade-offs among water, land, and crops within the oasis agricultural system of the Altay region. These include (1) an Agricultural Irrigation Water-Saving Scenario, which evaluates the water-saving potential of major crops by promoting efficient irrigation methods, referencing Xinjiang's agricultural water quotas and observed crop water requirements; (2) an Economic Crop Prioritization Scenario, aiming to maximize economic output per unit of water resource by simulating market-driven adjustments to crop planting structures and their effects on water and land resource efficiency; and (3) a forage crop prioritization scenario, which models the impact of transitioning traditional agriculture towards a forage-crop-dominated system on overall agricultural structure optimization and water and land resource allocation.

To ensure the simulation results are both practically feasible and offer valuable policy insights, this study established clear boundary conditions and constraints. Using 2023 as the baseline year, we integrated foundational data such as the acreage of major crops identified via remote sensing, along with their corresponding yields, prices, agricultural output value, and water consumption. For water resources, the total natural water availability of the rivers along the southern foothills of the Altay Mountains (1.02×10^{10} m^3) forms the basis, with a crucial constraint that agricultural water use will not exceed the current actual consumption of 1.471×10^9 m^3. Additionally, to prevent excessive expansion, the maximum planting area for major oasis crops is capped by the area extracted from 2023 remote sensing data. These rigorous settings ensure our simulations are firmly grounded in real-world data and existing constraints, thereby enhancing their relevance for regional water and land resource management policies.

Building on the established framework, we constructed a linear programming model for crop structure optimization. This model aims to maximize different objective functions under the constraint of total water resources, thereby revealing the variations in resource utilization efficiency and the inherent trade-off mechanisms associated with various development pathways. The formula is as follows:

$$W = \sum_{i=1}^{n} W_{\mathrm{i,irr}} \times A_{\mathrm{i}} \times C \tag{7}$$

In the equation, W represents the total regional water requirement (m^3); $W_{\mathrm{i,irr}}$ denotes the irrigation water requirement of the ith crop during its growing season (mm); and A_{i} is the planting area of crop i in square meters (m^2). C is a conversion factor (typically 0.001) to convert the irrigation depth from mm to m for consistency with the area unit.

In the context of an agricultural irrigation water-saving scenario, the objective function is to minimize the total agricultural water use. This can be formally expressed as follows:

$$\Delta W = W_{\mathrm{bi}} - W_{\mathrm{wq}} \tag{8}$$

In the equation, ΔW represents the water saved for the crop; W_{bi} is the baseline irrigation water requirement; and W_{wq} is the irrigation water requirement after implementing micro-irrigation measures. All values are in cubic meters (m^3).

In the Economic Crop Prioritization Scenario, to facilitate a more effective comparison of the economic value generated by different crops, the output value per unit area is calculated. This metric directly reflects the economic efficiency of each crop in terms of land utilization. The formula is as follows:

$$V = \sum_{i=1}^{n} Y_i \times P_i \quad (9)$$

In the equation, V represents the crop output value; Y_i is the unit yield of crop i (kg/km^2); and P_i is the market price of crop i (USD/kg).

To evaluate the water requirements of forage crops under various structural configurations, we calculate the total crop water demand for each specific crop structure scenario. The formula is as follows:

$$W_{cow} = A_{cow} \times W_{irr} \times C \quad (10)$$

In the equation, W_{cow} represents the irrigation water requirement per unit of beef cattle; A_{cow} is the required forage crop area per unit of beef cattle; and W_{irr} denotes the irrigation water requirement per unit area of forage crop. C is a conversion factor (typically 0.001) to convert the irrigation depth from mm to m for consistency with the area unit.

The maximum cultivable area for a specific crop, or a combination of crops, under a given water resource constraint can be calculated using the following general formula:

$$A_{crop} = \frac{W_{crop}}{W_{irr}} \quad (11)$$

In the equation, A_{crop} represents the planting area of the crop (hm^2); W_{crop} denotes the allocated irrigation water volume for the crop (m^3); and W_{irr} is the irrigation water requirement per unit area of the crop (mm).

3. Results

3.1. Spatiotemporal Characteristics of Oasis and Land Use

As shown in Figure 4a, the total area of oasis regions in Altay Prefecture in 2023 was approximately 14,015 km^2, primarily located in low-altitude piedmont plains and river valley depressions. According to Figure 4b, the Ulungur River basin had the largest oasis area, accounting for 27.4%, followed by the Kran River and Haba River basins, which accounted for 22.16% and 10.82%, respectively. Figure 4c illustrates that the dominant land-cover types in oasis areas were cropland and grassland, with areas of 5364.62 km^2 and 5308.21 km^2, respectively, together comprising 76.2% of the total area. These were followed by water (1437.23 km^2) and bare land (1806.36 km^2), while built-up land and forestland covered 46.44 km^2 and 52.15 km^2, respectively. Cropland was mainly distributed in the Kran River and Ulungur River basins, jointly accounting for 45.5% of the total. Grassland was primarily located in the Haba River and Kran River basins. Water in the Ulungur River basin accounted for 83.7% of the total water area in oasis regions, while bare land was mainly distributed in the Ulungur and Haba River basins (Figure 4).

3.2. Spatiotemporal Characteristics of Major Crops in the Oasis

As shown in Figure 5a, the planting areas of major crops in Altay Prefecture in 2023 were sunflower (1241 km^2), spring maize (1410 km^2), spring wheat (377 km^2), and alfalfa (340 km^2), collectively occupying 3368 km^2 and representing 78.17% of the total cropland. Extracting the planting areas of these major crops helps reveal the cropping structure and spatial distribution of oasis agriculture. According to Figure 5b, the major crops were mainly distributed in the middle and lower reaches of the Ulungur River, its internal basin, and the Kran River basin. Figure 5c indicates that the highest proportions of sunflower cultivation were observed in the Kara Irtysh River basin, the internal basin of the Ulungur River, and its middle and lower reaches. In other basins, spring maize was the dominant crop. Higher proportions of spring wheat cultivation were found in the Kara Irtysh,

Berezek, and Burqin River basins, while alfalfa was more commonly planted in the Haba and Berezek River basins (Figure 5).

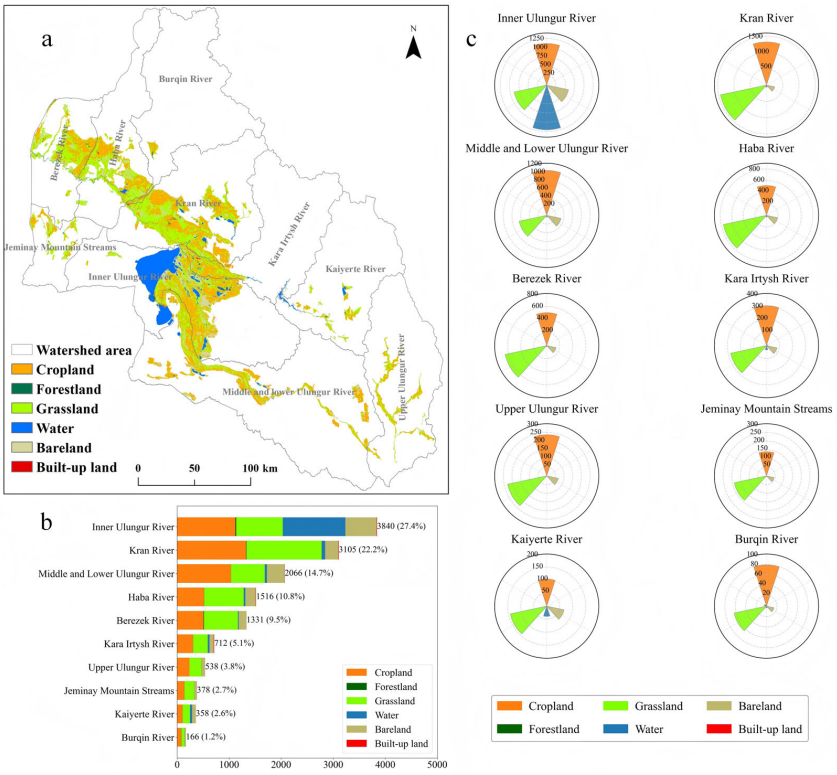

Figure 4. Spatial patterns of oasis land cover in Altay Prefecture in 2023. (**a**) Spatial distribution of land cover in oasis. (**b**) Distribution by basins in oasis. (**c**) Land-cover structure by basins in oasis.

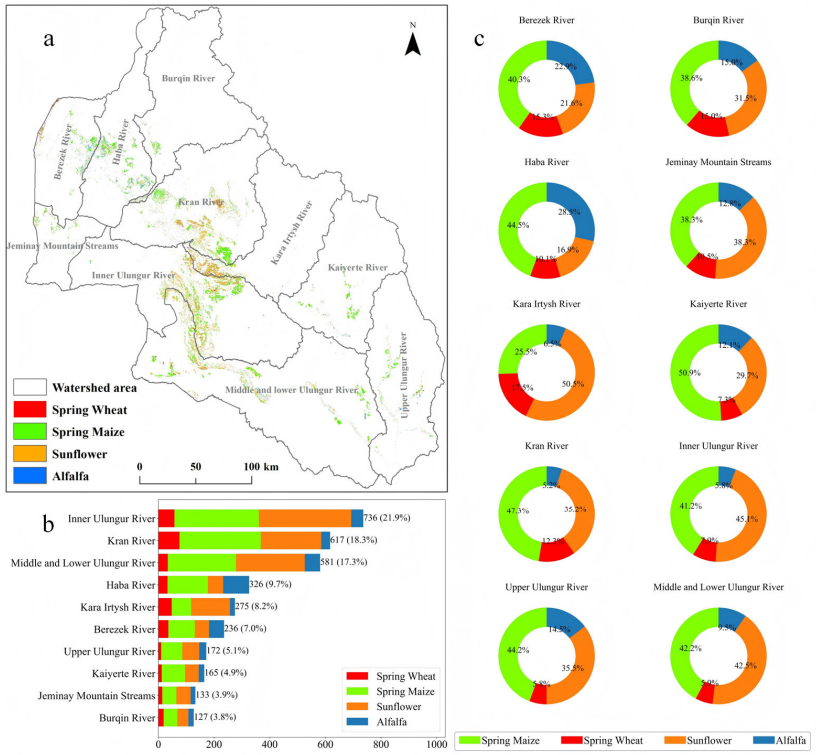

Figure 5. Cropping structure of major crops in the oasis of Altay Prefecture in 2023. (**a**) Spatial distribution of major crops in oasis. (**b**) Crop distribution by basins. (**c**) Crop planting structure by basins.

3.3. Water Requirement Characteristics of Major Crops

3.3.1. Crop Water Requirements During Growth Periods for Major Crops

As a major component of water consumption in arid regions, the accurate estimation of crop water requirements provides an effective pathway for precise water resource management and quantification. This also contributes to a comprehensive understanding of water-use characteristics in agricultural production zones. Based on Equations (2) and (3), the crop water requirements over the full growing period for major crops in Altay Prefecture were calculated using 44 years of daily average meteorological data from regional weather stations, in conjunction with crop coefficients and growth stages.

As shown in Figure 6, the long-term average crop water requirements for spring wheat, alfalfa, spring maize, and sunflower were 594 mm, 590 mm, 550 mm, and 450 mm, respectively. Among the different crop types, spring wheat had the highest water demand, while sunflower had the lowest. Spatially, the distribution exhibits a west-to-east decreasing trend along the longitudinal direction, with Qinghe County showing lower values due to its higher elevation and reduced evaporation. Latitudinally, a south-to-north decreasing trend is observed, primarily because the southern areas are low-lying plains with higher evaporation, whereas the northern areas are mountainous (Figure 6).

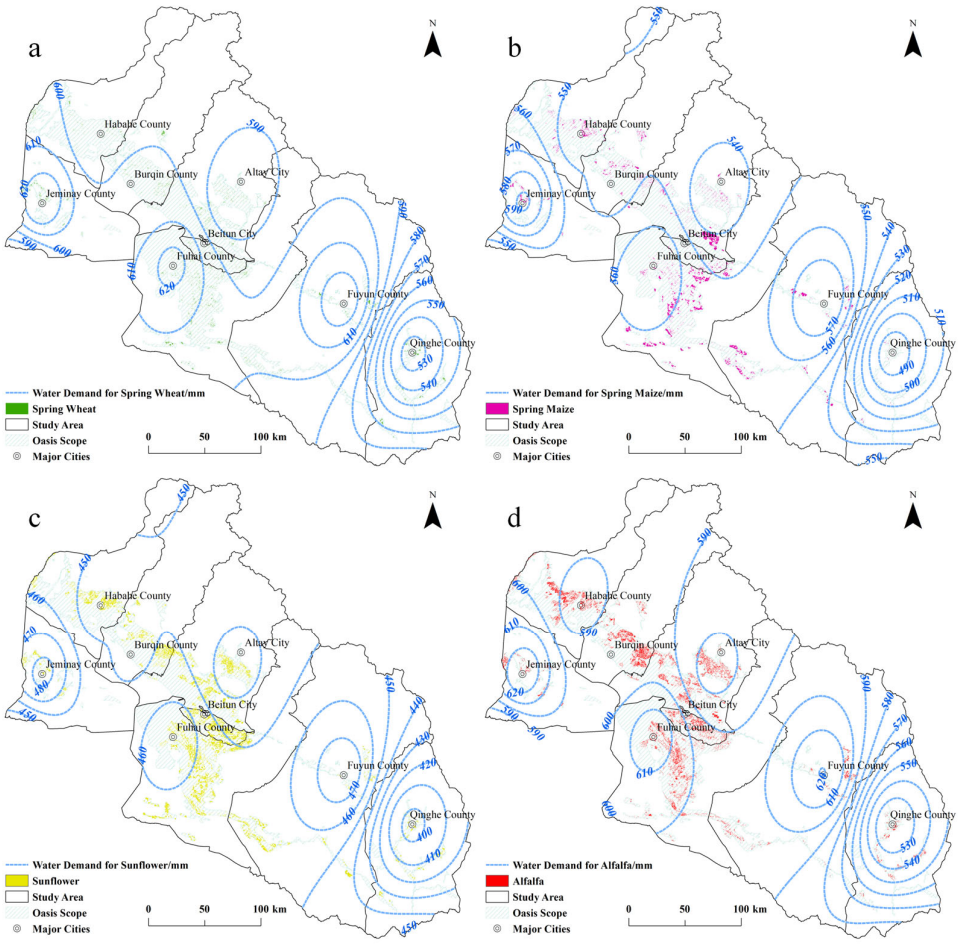

Figure 6. The average water requirement during the growth period of crops in the oasis of Altay Prefecture. (**a**) Long-term average crop water requirement for spring wheat. (**b**) Long-term average crop water requirement for spring maize. (**c**) Long-term average crop water requirement for sunflower. (**d**) Long-term average crop water requirement for alfalfa.

3.3.2. Effective Precipitation During Growth Periods for Major Crops

Sufficient water supply is essential to meet the crop water demand during the growing period. In general, crop water needs are met by natural precipitation. Effective precipitation refers to the portion of rainfall that can be directly absorbed by crops. To accurately estimate effective precipitation during the crop growing period, Equation (4) was applied to calculate the effective precipitation for major oasis crops in Altay Prefecture.

As shown in Figure 7, the multi-year average effective precipitation for spring maize, alfalfa, spring wheat, and sunflower over the full growing season was 86 mm, 86 mm, 84 mm, and 84 mm, respectively. This indicates a severe deficiency of effective precipitation during the crop growing period, with precipitation satisfaction rates as low as 15%, which is far from sufficient to meet crop water requirements. Spring maize and alfalfa received slightly more effective precipitation than spring wheat and sunflower. Daily precipitation during the growing period showed minimal variation. This difference was primarily influenced by the length of the growing period. Spatially, a distinct pattern of low values in the central region and higher values in peripheral areas was observed, precipitation in high-altitude areas was significantly greater than in low-altitude counties (Figure 7).

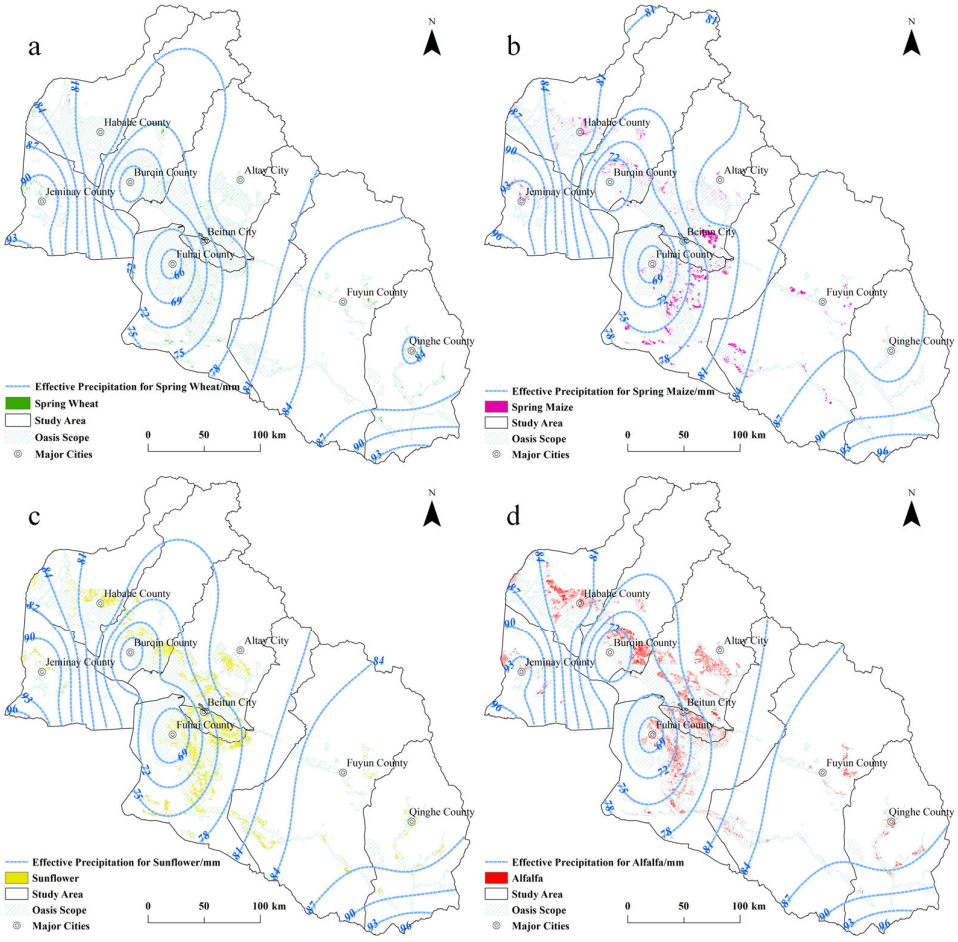

Figure 7. The average effective precipitation during the growth period of crops in the oasis of Altay Prefecture. (**a**) Long-term average effective precipitation for spring wheat. (**b**) Long-term average effective precipitation for spring maize. (**c**) Long-term average effective precipitation for sunflower. (**d**) Long-term average effective precipitation for alfalfa.

3.3.3. Crop Irrigation Water Requirements During Growth Periods for Major Crops

Given the severe insufficiency of natural precipitation during the crop growing period in the oasis areas of Altay Prefecture, agricultural irrigation has become the primary source

of water to sustain crop growth. The irrigation water requirement is generally defined as the supplementary water needed during the growing period, calculated by subtracting the effective precipitation from crop water demand. Using Equation (5), the irrigation water requirements for major oasis crops in Altay Prefecture were calculated.

As shown in Figure 8, the multi-year average irrigation requirement over the full growing period for spring wheat, alfalfa, spring maize, and sunflower was 510 mm, 504 mm, 464 mm, and 365 mm, respectively. Spring wheat had the highest irrigation requirement, while sunflower had the lowest. Irrigation demand showed strong spatial consistency with crop water demand. Spatially, irrigation demand exhibited a west-to-east decreasing trend along the longitude and a south-to-north decreasing trend along the latitude (Figure 8).

For calculation simplicity, we used the average crop coefficients for the entire growth period. The crop water requirement, effective precipitation, and irrigation water requirement were all computed using daily crop meteorological data (Table 4).

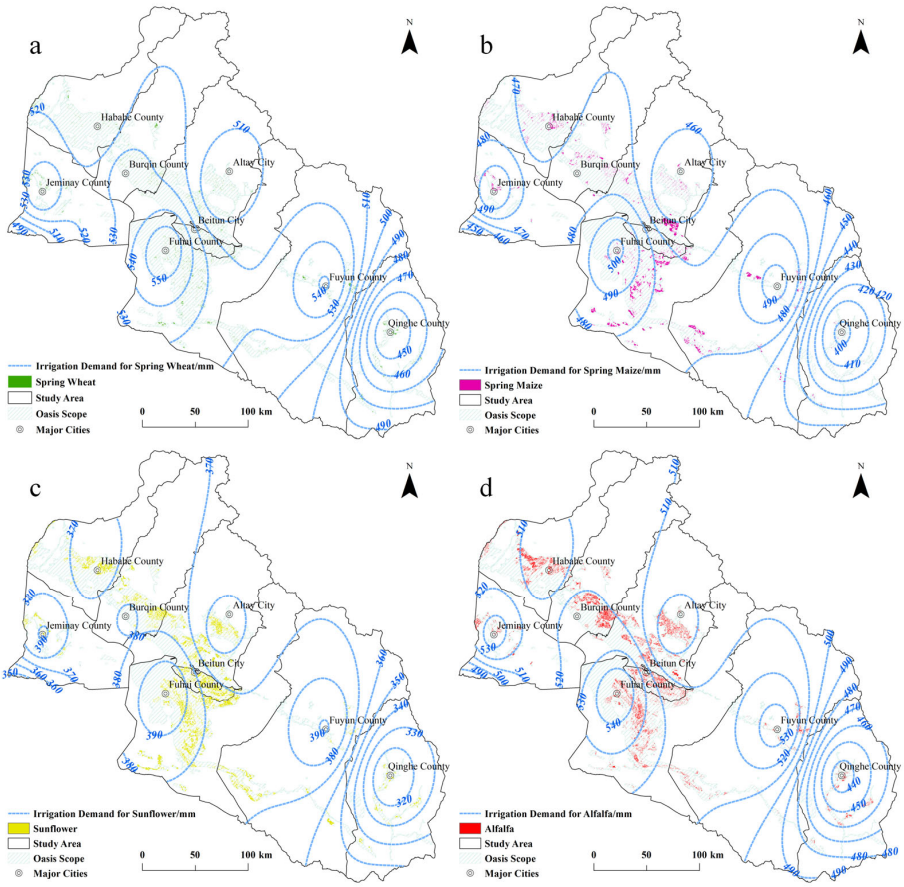

Figure 8. The average irrigation water requirement during the growth period of crops in the oasis of Altay Prefecture. (**a**) Long-term average irrigation water requirement for spring wheat. (**b**) Long-term average irrigation water requirement for spring maize. (**c**) Long-term average irrigation water requirement for sunflower. (**d**) Long-term average irrigation water requirement for alfalfa.

Table 4. Water requirement characteristics of main crops in the oasis of Altay Prefecture.

Crop Type	Crop Coefficient	Crop Water Requirement (mm)	Effective Precipitation (mm)	Irrigation Water Requirement (mm)
Spring Wheat	0.92	594	84	510
Spring Maize	0.90	550	86	464
Sunflower	0.85	449	84	365
Alfalfa	0.94	590	86	504

3.4. Water Consumption by Crops

The major crops cultivated, including sunflower (1241 km^2), spring maize (1410 km^2), spring wheat (377 km^2), and alfalfa (340 km^2), cover a total area of 3368 km^2. The combined total irrigation water demand for these crops is 1.471 $\times$ 10^9 m^3, broken down as follows: sunflower (1.73 $\times$ 10^8 m^3), spring maize (6.54 $\times$ 10^8 m^3), spring wheat (4.53 $\times$ 10^8 m^3), and alfalfa (1.90 $\times$ 10^8 m^3) (Table A1). Agricultural water consumption reaches 2.675 $\times$ 10^9 m^3, accounting for 82.5% of the regional total water use. Notably, the major crops occupy only 2.85% of the land area yet account for 26.23% of the region's water consumption, highlighting the structural contradictions in the use of agricultural water and land resources. Given the significant impact of agricultural water use on regional water resources and based on the characteristics of agricultural water and land resources in the Altay oasis, this study proposes a multi-scenario simulation analysis approach to explore effective strategies for reducing agricultural water and land resource consumption, aiming to provide decision-making guidance for the management and optimization of water and land resources in the region.

3.5. Multi-Scenario Trade-Off Analysis of Water–Land Resource Utilization

3.5.1. Scenario of Agricultural Irrigation Water Conservation

Based on the agricultural water quotas and measured crop water requirements in Xinjiang, this study quantifies the water-saving effects of drip irrigation technology. After adopting drip irrigation water-saving measures, the water savings per unit area for spring wheat, alfalfa, and spring maize are 155 mm, 126 mm, and 59 mm, respectively, while sunflower, with a lower water consumption under conventional irrigation, can still save 25 mm per unit area (Table A2).

If micro-irrigation water-saving techniques are widely adopted for all major crops, the total water savings for the current crop areas could reach 2.14 $\times$ 10^8 m^3, with spring maize contributing the largest share of 0.83 $\times$ 10^8 m^3, accounting for 38.8%, which is related to its large planting area. Alfalfa and spring wheat contribute 0.48 $\times$ 10^8 m^3 and 0.53 $\times$ 10^8 m^3, respectively, accounting for 22.1% and 24.6%. Sunflower water savings amount to 0.31 $\times$ 10^8 m^3, accounting for 14.5%.

Spring wheat and alfalfa, being high-water-demand crops, show the greatest reduction in water consumption per unit area after implementing water-saving measures. Therefore, they should be prioritized for water-saving transformations. Spring maize, with the largest planting area, has significant overall water-saving potential. Strengthening water-saving measures for spring maize on a large scale can significantly increase agricultural water savings.

Moreover, if micro-irrigation technology is promoted for major crops, under current water resource consumption, the total planting area for major crops (sunflower, spring maize, spring wheat, and alfalfa) could expand to 3931 km^2, based on existing planting proportions. This represents a significant 16.72% increase in cultivable land.

3.5.2. Scenario of Prioritizing Cash Crops

This study quantitatively assesses the coupling of water and land resources under a prioritization of economic crops in the Altay oasis, this study quantitatively evaluates the coupling status of water and land resources under a target-oriented strategy that prioritizes the cultivation of economic crops. As can be seen from the table, silage maize has the highest yield per unit area, yet its economic value is lower than that of edible sunflower. Although edible sunflower has relatively lower yields, it generates the highest economic return among the crops. This suggests that expanding the cultivation area of high-value

crops such as edible sunflower could significantly enhance the agricultural output value in the region (Table A3).

Under the constraints of current water resource consumption, if crop planting areas were allocated based on normalized economic value proportions, the optimized planting areas for major oasis crops would be as follows: spring wheat at 335 km^2, spring maize at 483 km^2, silage maize at 663 km^2, edible sunflower at 1175 km^2, oilseed sunflower at 607 km^2, and alfalfa at 238 km^2. The total planting area would remain almost unchanged from the current status, but there would be a significant increase in the planting areas for edible sunflower and oilseed sunflower. This results in a total cultivated area of 3492 km^2, representing a 3.56% increase from the current state, with a notable expansion in sunflower cultivation. If water-saving technologies are implemented, the total cultivated area could further increase to approximately 4025 km^2, with corresponding areas of spring wheat at 481 km^2, grain maize at 553 km^2, silage maize at 760 km^2, edible sunflower at 1262 km^2, oil-use sunflower at 653 km^2, and alfalfa at 317 km^2. This represents a substantial 15.3% increase. Specifically, if the primary crops were entirely adjusted to edible sunflower, the planting area for edible sunflower would increase to 4030 km^2, representing an expansion of approximately 662 km^2 or 19.65% compared to the current situation. After applying water-saving measures, this area could extend to 4327 km^2, showing a 7.36% increase. These findings suggest that expanding edible sunflower cultivation can lead to both an increased planting area and enhanced agricultural output value.

When optimizing planting under the constraints of the current planting areas, if crop planting areas were allocated based on normalized economic value proportions, the optimized areas for the main oasis crops would be approximately as follows: spring wheat at 389 km^2, grain maize at 513 km^2, silage maize at 704 km^2, edible sunflower at 982 km^2, oil-use sunflower at 506 km^2, and alfalfa at 274 km^2. The total water consumption would be 1.445×10^9 m^3, reflecting a reduction of 0.28×10^8 m^3 or 1.89% compared to the original system. Furthermore, with the application of water-saving technologies, total water consumption could drop to 1.241×10^9 m^3, a 14.1% reduction. If the primary crops were exclusively adjusted to edible sunflower, the total water consumption would decrease to 1.229×10^9 m^3, representing a reduction of 2.42×10^8 m^3 or 16.45% compared to the original cropping system. After implementing water-saving technologies, the total water consumption would be 1.145×10^9 m^3, showing a 6.85% decrease compared to the "edible sunflower only" scenario without water-saving tech. These findings demonstrate that expanding the cultivation area of edible sunflower can effectively reduce agricultural water consumption and significantly enhance the water-use efficiency in oasis agriculture.

3.5.3. Scenario of Prioritizing Forage Crops

This study simulates and evaluates the water and land resource coupling in the Altay oasis, focusing on a forage crop prioritization scenario under existing water and land resource constraints. For a single beef cattle life cycle, the cultivation area required for four types of forage crops is approximately 2933.35 m^2, with a corresponding water consumption of about 1243 m^3. However, the low yield and high water consumption of soybeans imply that sourcing from outside the region may be more efficient. Excluding soybean, the planting area for the remaining three forage crops is approximately 2000 m^2, with water consumption reduced to about 955 m^3, representing a 23% decrease (Table A4).

Under the current water resource constraints, allocating land according to the demand structure of four forage crops would require a total planting area of approximately 3479 km^2, which is slightly higher than the current level and could support feed demand for approximately 1.1834×10^6 beef cattle. Implementing water-saving technologies would further expand the planting area to 4317 km^2, an impressive 19.2% increase. In contrast,

allocating based on the demand structure of only three forage crops would reduce the required planting area to about 3080 km^2 and could support feed demand for approximately 1.54 × 10^6 beef cattle. Compared with the four-crop system, the latter increases the breeding capacity by 3.57 × 10^5 cattle, a 30% improvement. Applying water-saving technologies would boost the planting area to 3699 km^2, a 20.16% increase. These results suggest that adjusting the forage crop composition has the potential to significantly expand the region's livestock production capacity.

Under the constraint of existing arable land, adopting a four-crop forage structure would result in a water consumption of 1.43 × 10^9 m^3, which is slightly lower than that of the original cropping pattern and sufficient to feed approximately 1.15 × 10^6 beef cattle. When water-saving technologies are applied, total water consumption reduces to 1.191 × 10^9 m^3, a 16.66% decrease. In contrast, adopting a three-crop structure (excluding soybean) would lead to a water consumption of 1.61 × 10^9 m^3, an increase of 9%, and could meet the feed demand of approximately 1.68 × 10^6 cattle. Compared to the former system, this represents a 1.79 × 10^8 m^3 (12.5%) increase in water use and also an increase in breeding capacity of 5.35 × 10^5 cattle, or 46.45%. With water-saving technologies, the total water consumption would be 1.334 × 10^9 m^3, a 16.93% decrease.

Notably, under the same water consumption level, the three-crop system (excluding soybean) can still support feed demand for approximately 1.50 × 10^6 cattle, 30.2% more than the four-crop system. These findings indicate that the three-crop combination, excluding soybean, has significant potential to increase the upper limit of regional livestock capacity.

Through comparative analysis of multiple scenarios, the study systematically demonstrates the differences in crop planting areas, agricultural water demand characteristics, and potential water savings under three simulated scenarios, revealing the utilization patterns of regional agricultural land and water resources under different management strategies (Figures 9 and 10).

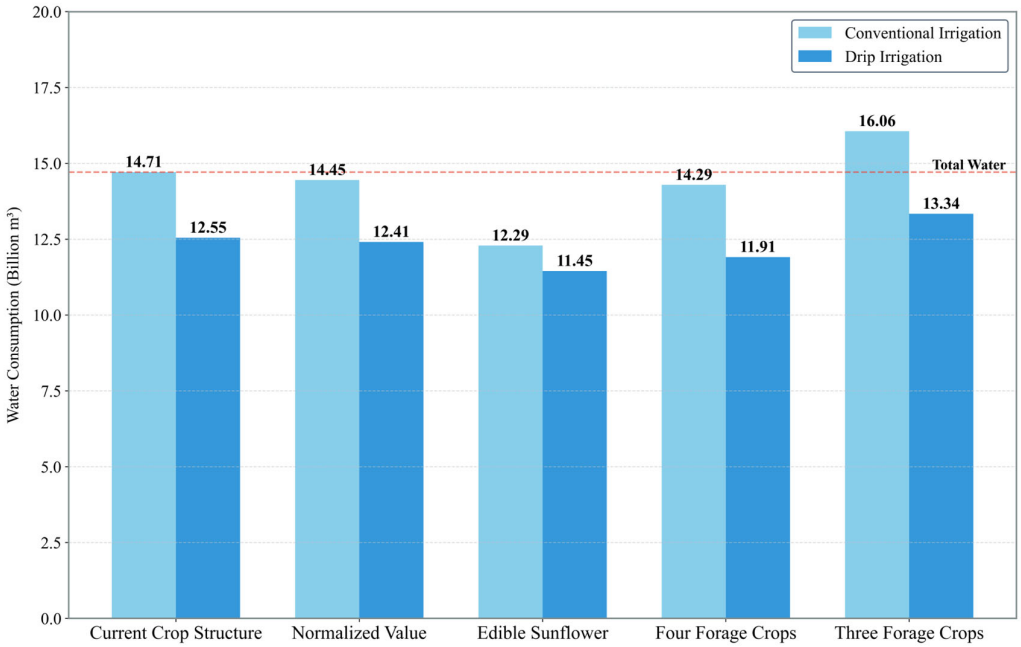

Figure 9. Water consumption under various scenarios.

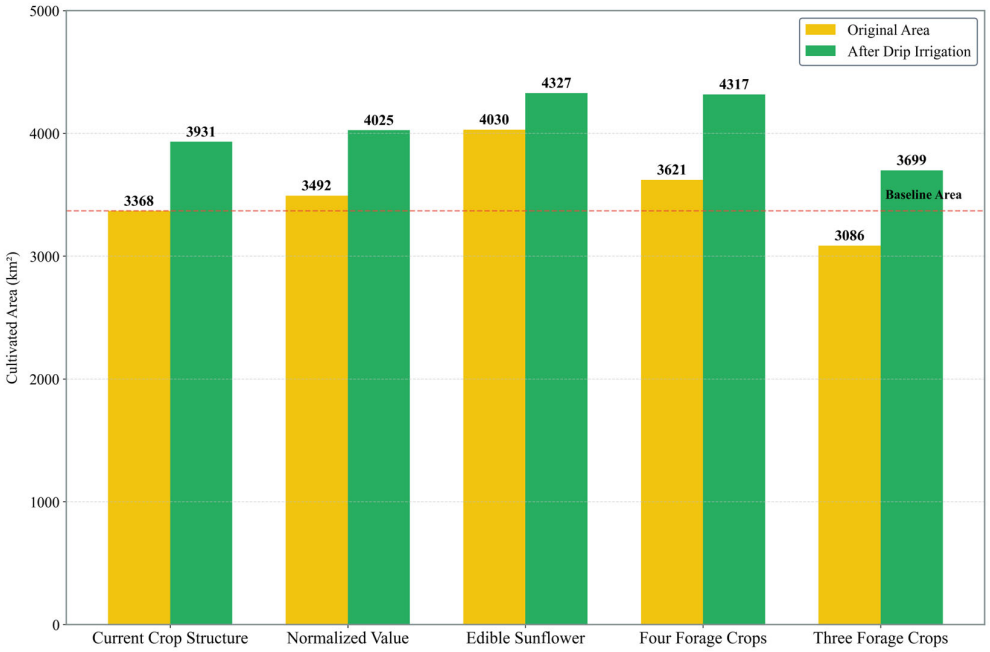

Figure 10. Crop planting area under various scenarios.

4. Discussion

This study introduces a novel, integrated research framework that combines remote sensing identification, water demand modeling, and multi-scenario optimization. This framework offers a fresh perspective and powerful tools for managing water and land resources in arid oasis agriculture, particularly in exploring the coupling relationship between land and water resources in the Altay oasis, which is vital for sustainable management in arid regions. Leveraging this framework, we successfully developed a crop identification model applicable at the regional scale, significantly enhancing the spatiotemporal resolution of crop water requirement estimations. Furthermore, we simulated and evaluated the dynamic changes in water and land resources under various development scenarios. This comprehensive approach provides a robust scientific basis for the optimized allocation of regional water and land resources.

Through this integrated framework, we first leveraged the Google Earth Engine (GEE) to rapidly construct crop spectral and vegetation index time-series curves [76] and developed a large-scale crop identification model with significantly improved spatial and temporal accuracy. The crop planting structure in the study area is clearly dominated by spring maize and sunflower, which together account for a significant 79.3% of the total major crop area. This approach not only boosted research efficiency but also provided the necessary technical support for large-scale, high-precision crop identification [77–79]. This precision in remote sensing identification is a cornerstone of our integrated framework, directly feeding into accurate water demand estimations.

Existing research consistently shows that agricultural water use in arid regions often exceeds 80% of total water consumption, frequently coupled with inefficient water allocation [62]. This reinforces the significant reliance of oasis agriculture on irrigation and highlights a clear imbalance in water resource distribution. This study delves deeper by quantifying the differences in water resource utilization among various crop types. We found that spring wheat and alfalfa have higher water requirements during their growing seasons compared to spring maize and sunflower. This observation is directly linked to the crops' physiological characteristics. Spring wheat's longer growth period and higher transpiration rates and alfalfa's multi-cutting cycles both contribute to their elevated water needs. In contrast, sunflower exhibits superior water-saving performance due to its

strong drought resistance and shorter growing period, alongside a promising potential for economic output.

As seen in Table A5, our study's crop water requirement (CWR) values for spring wheat (594 mm) and spring maize (550 mm) generally align with the upper range of existing studies in similar climatic regions. Comparing our findings with diverse regional studies, crop water demand shows considerable variability, underscoring the critical influence of local climate, specific crop characteristics, and methodological approaches. For example, reported wheat CWRs range from around 427–693 mm in northern Algeria to 511–548 mm in Xinjiang, China, while maize CWRs vary from 350 to 380 mm in Xinjiang to 552 mm in Northeast China. Similarly, evapotranspiration (ET) for sunflower (638–882 mm) and alfalfa (up to 1427 mm) highlights their significant water consumption in different contexts. These variations emphasize that relying solely on generalized data can be misleading for water management. Our integrated framework, however, precisely accounts for these regional specificities, providing tailored and accurate CWR estimations crucial for effective water resource management [44,71,73,80–87].

Our findings, indicating that effective precipitation meets less than 15% of crop water demand during the growing season, further confirm this high dependence on irrigation in the region. By integrating these water demand insights into our multi-scenario analysis, we propose sunflower as an optimal choice for a water-saving economic crop. This offers new evidence and a clear direction for achieving a synergistic optimization of a "water-food-economy" in arid regions.

Our research, facilitated by the holistic capabilities of the integrated framework, reveals several critical insights for sustainable agricultural development in arid regions. Promoting water-saving technologies can unlock nearly 2×10^8 m^3 of water-saving potential. Notably, spring wheat and alfalfa offer the largest water-saving potential per unit area, providing clear priority areas for future agricultural water conservation policies. When optimizing planting structures based on the principle of maximizing economic output, our model shows a significant expansion in edible sunflower cultivation. Crucially, this expansion leads to a reduction in regional water consumption while simultaneously increasing agricultural output value. This confirms that intelligent crop structure optimization can substantially boost water resource efficiency and agricultural economic growth [88]. It is also noteworthy that optimizing forage crop planting structures not only reduces the water demand for beef cattle feed but also helps to increase the livestock farming scale. This clearly demonstrates the immense potential of forage crops in the agricultural transformation of arid regions. This finding further validates the "forage crop substitution strategy" proposed in this study as a feasible and important approach for ecologically vulnerable areas, offering new avenues for building more resilient agro-pastoral composite systems.

Despite the positive results, this study acknowledges limitations, primarily the constraint of mixed pixels on small-plot crop classification accuracy due to remote sensing image resolution, where small fields or their edges may contain multiple crop types, affecting precision. Future research should address this by integrating more vegetation indices for comprehensive analysis and incorporating deep learning algorithms that combine a time-series NDVI/EVI, spectral features, and texture information to build multi-modal crop identification models, thereby significantly enhancing classification accuracy [89–94].

Our current estimations of crop water requirements face challenges primarily due to the limited distribution of meteorological stations, leading to data gaps in mountainous and other complex terrains, which can affect accuracy [95]. Furthermore, while the crop coefficient (Kc) values are largely sourced from the existing literature, we have incorporated local field experiment results for calibration [96–101]. To enhance the real-time accuracy and spatial adaptability of crop water requirement estimations, future research

should focus on developing a more precise and dynamic Kc database. This could be achieved through remote sensing inversion techniques or by establishing a denser network of onsite observations.

While the promotion of micro-irrigation technologies like drip irrigation offers significant reductions in water usage per unit area, a substantial hurdle is the high upfront infrastructure investment [102]. The water-saving benefits often require several years of operation to recoup these initial costs. Similarly, though economic crops can yield 2–3 times the output value of traditional crops per unit area, their large-scale expansion carries potential risks. This could lead to market supply–demand imbalances and increased ecological vulnerability, such as depleted soil fertility and a heightened risk of pests and diseases [103–106]. Furthermore, optimizing the structure of forage crop cultivation necessitates establishing stable external supply channels. This is crucial to ensure the consistency of forage supply and to reduce the region's dependence on internal production alone.

Finally, our scenario settings were based on fixed market conditions and policy environments. This approach did not fully account for the complex influence of market and policy dynamics on farmers' planting decisions, such as fluctuations in agricultural product prices or changes in water resource management policies and subsidies. Agricultural decisions are typically the result of an intricate interplay of multiple factors, including climate change, the speed of technology adoption, and dynamic market demands [107–112]. Therefore, future research could incorporate socio-ecological models (SESs) or probabilistic scenario analysis [113,114]. This would enhance the dynamism and adaptability of scenario analysis, allowing for a more comprehensive simulation and evaluation of the complex behaviors within agricultural systems and thus a more robust exploration of the coupling relationship between land and water resources.

5. Conclusions

This study successfully developed an integrated framework combining remote sensing, a crop water model, and multi-scenario analysis to explore the coupling relationship between land and water resources in Altay's oasis agriculture. Our research yielded several key findings.

Firstly, a significant achievement of this research was demonstrating that the decision tree method can effectively identify crops at a regional scale using remote sensing data. This capability provides the foundational, precise crop distribution data essential for accurate water resource assessment within our integrated framework. We also found a dominance of a few major crops—spring wheat, spring maize, sunflower, and alfalfa—which together account for over 78% of the total sown area. Secondly, the framework enabled the accurate quantification of crop water requirements, a vital input for water resource management. Our precise crop water modeling identified that spring wheat and alfalfa exhibit the highest water demand, while sunflower shows strong water-saving potential and economic benefits. Natural precipitation meets only 15% of crop water needs, highlighting the Altay oasis's heavy reliance on irrigation. Despite occupying only 2.85% (3368 km^2) of the total land area, the main crops account for 82.5% of total regional water use. This highlights the need for targeted water management strategies tailored to these high-impact crops. Furthermore, through multi-scenario simulation and analysis, the framework effectively identified strategies for both water conservation and agricultural development. Promoting micro-irrigation technology and expanding sunflower cultivation can significantly reduce agricultural water consumption while increasing the agricultural output value. Optimizing forage crop structures offers substantial dual benefits for both livestock development and water conservation. Specifically, prioritizing a three-crop forage system (excluding soybean) significantly enhanced beef cattle breeding capacity, even under existing land or

water constraints. This strategic shift in forage cultivation directly supports expanding the livestock scale while simultaneously conserving precious water resources.

In conclusion, by synergistically linking remote sensing, water modeling, and scenario analysis, this study offers a more holistic and accurate basis for sustainable decision-making than traditional, fragmented methods. This study not only advances an academic understanding of land and water resource optimization in arid agriculture but also provides a scientific basis for sustainable water and land resource management in arid oasis regions.

Author Contributions: Conceptualization, G.Y. and L.J.; methodology, G.Y. and L.J.; formal analysis, L.J.; resources, Y.L.; data curation, G.Y. and Y.L.; writing of original draft, G.Y. and L.J.; writing—review and editing, L.J.; supervision, L.J.; project administration, L.J.; funding acquisition, L.J. All authors have read and agreed to the published version of the manuscript.

Funding: This research was funded by the Third Xinjiang Comprehensive Scientific Expedition Program, grant number 2022xjkk0803, and the National Natural Science Foundation of China, grant number 42071253.

Data Availability Statement: This study employed daily meteorological data from ten meteorological stations around Altay Prefecture, obtained from the China Meteorological Data Service Center (https://data.cma.cn. accessed on 13 August 2023). Oasis data were obtained from the National Glacial, Permafrost and Desert Scientific Data Center (http://www.ncdc.ac.cn. accessed on 13 April 2023).

Acknowledgments: The authors are grateful to the reviewers for their comments and suggestions.

Conflicts of Interest: The authors declare no conflicts of interest.

Appendix A

Table A1. The amount of water resources consumed by the main crops in the oases of Altay Prefecture.

Crop Type	Area/hm^2	Irrigation Water Requirement/mm	Total Water Requirement/m^3
Spring Wheat	340	510	1.73×10^8
Spring Maize	1410	464	6.54×10^8
Sunflower	1241	365	4.53×10^8
Alfalfa	377	504	1.90×10^8
Total	3368	1843	14.71×10^8

Table A2. Water consumption and water-saving potential of crops in Altay Prefeture's oasis under different irrigation methods.

Crop Type	Conventional Irrigation Water Requirement/mm	Micro-Irrigation Water Requirement/mm	Water Savings/m^3
Spring Wheat	510	355	0.53×10^8
Spring Maize	464	405	0.83×10^8
Sunflower	365	340	0.31×10^8
Alfalfa	504	378	0.48×10^8

Table A3. Prices of crop products in the oasis of Altay Prefecture.

	Spring Wheat	Spring Maize	Silage Maize	Edible Sunflower	Oilseed Sunflower	Alfalfa
Yield (kg/hm^2)	629,070	881,610	7,792,500	317,655	317,655	823,245
Price (USD/kg)	0.36	0.34	0.05	1.81	0.93	0.20
Value (USD/hm^2)	226,465.20	299,747.40	389,625.00	574,955.55	295,419.15	164,649.00

Table A4. Feed structure of beef cattle.

Feed Composition	Crop Type	Demand/kg	Yield/kg	Required Area/m^2	Irrigation Water Requirement/mm
Concentrated Feed	Spring maize	600	600	666.67	464
	Soybean	250	182	933.34	309
Roughage	Silage maize	4000	4000	666.67	464
	Forage crops	1000	1000	666.67	504

Table A5. Comparison of crop water requirements.

Study Region	Research Subject	Method	CWR/mm	ET/mm
Xinjiang, China	Wheat	Penman-Monteith	511–548	
Northern Algeria	Wheat	CROPWAT	427–693	
Xinjiang, China	Summer Maize	Penman-Monteith	350–380	
Songhua River Basin, China	Maize, Soybean	Penman-Monteith	463.64, 396.48	
China	Maize	Penman-Monteith	105–486	
Yellow River Basin, China	Winter wheat	Penman-Monteith	540	
Northeast China	Maize	Penman-Monteith	552	
Beka Valley of Lebanon	Sunflower	Lysimeter		765–882
US Southern High Plains	Sunflower	Lysimeter		638
Arizona, USA	Wheat, Alfalfa	Remote sensing		742, 1427
Gansu Province, China	Alfalfa	Penman-Monteith	700	

References

1. He, Y.X.; Liu, C.F.; Ni, B.; Lian, H.G. Ecological Network Resilience of Shiyang River Basin: An Arid Inland Watershed of Northwest China. *Chin. Geogr. Sci.* **2024**, *34*, 951–966. [CrossRef]
2. Zhang, Q.; Sun, C.; Chen, Y.; Chen, W.; Xiang, Y.; Li, J.; Liu, Y. Recent Oasis Dynamics and Ecological Security in the Tarim River Basin, Central Asia. *Sustainability* **2022**, *14*, 3372. [CrossRef]
3. Cui, B.; Gui, D.; Liu, Q.; Abd-Elmabod, S.K.; Liu, Y.; Lu, B. Distribution and Growth Drivers of Oases at a Global Scale. *Earths Future* **2024**, *12*, e2023EF004086. [CrossRef]
4. Zhang, Z.; Xu, E.; Zhang, H. Complex Network and Redundancy Analysis of Spatial–Temporal Dynamic Changes and Driving Forces behind Changes in Oases within the Tarim Basin in Northwestern China. *Catena* **2021**, *201*, 105216. [CrossRef]
5. Chen, B.; Duan, Q.; Zhao, W.; Wang, L.; Zhong, Y.; Zhuang, Y.; Chang, X.; Dong, C.; Du, W.; Luo, L. Oasis Sustainability Is Related to Water Supply Mode. *Agric. Water Manag.* **2023**, *290*, 108589. [CrossRef]
6. Pokhrel, Y.; Felfelani, F.; Satoh, Y.; Boulange, J.; Burek, P.; Gaedeke, A.; Gerten, D.; Gosling, S.N.; Grillakis, M.; Gudmundsson, L.; et al. Global Terrestrial Water Storage and Drought Severity under Climate Change. *Nat. Clim. Change* **2021**, *11*, 226–233. [CrossRef]
7. Liu, K.; Li, X.; Wang, S.; Zhou, G. Past and Future Adverse Response of Terrestrial Water Storages to Increased Vegetation Growth in Drylands. *npj Clim. Atmos. Sci.* **2023**, *6*, 113. [CrossRef]
8. Liu, X.; Tang, Q.; Zhao, Y.; Wang, P. Persistent Water Scarcity due to High Irrigation Demand in Arid China: A Case Study in the North Slope of the Tianshan Mountains. *Earths Future* **2024**, *12*, e2024EF005070. [CrossRef]
9. Daramola, M.T.; Xu, M. Recent Changes in Global Dryland Temperature and Precipitation. *Int. J. Climatol.* **2022**, *42*, 1267–1282. [CrossRef]
10. Fan, B.; Shi, X.; Luo, G.; Hellwich, O.; Ma, X.; Shang, M.; Wang, Y.; Ochege, F.U. Ground Subsidence and Disaster Risk Induced by Groundwater Overexploitation: A Comprehensive Assessment from Arid Oasis Regions. *Int. J. Disaster Risk Reduct.* **2025**, *119*, 105328. [CrossRef]
11. Chen, B.; Liu, S.; Yu, S.; Chen, W.; He, X.; Wang, Y. Cropland Expansion Is Threatening Terrestrial Water Storage in Dryland Watersheds. *J. Clean. Prod.* **2025**, *501*, 145333. [CrossRef]
12. Li, H.; Li, Z.; Chen, Y.; Xiang, Y.; Liu, Y.; Kayumba, P.M.; Li, X. Drylands Face Potential Threat of Robust Drought in the CMIP6 SSPs Scenarios. *Environ. Res. Lett.* **2021**, *16*, 114004. [CrossRef]
13. Asadnabizadeh, M. Critical Findings of the Sixth Assessment Report (AR6) of Working Group I of the Intergovernmental Panel on Climate Change (IPCC) for Global Climate Change Policymaking a Summary for Policymakers (SPM) Analysis. *Int. J. Clim. Change Strateg. Manag.* **2023**, *15*, 652–670. [CrossRef]

14. Wang, H.; Liu, Y.; Wang, Y.; Yao, Y.; Wang, C. Land Cover Change in Global Drylands: A Review. *Sci. Total Environ.* **2023**, *863*, 160943. [CrossRef]
15. Peng, Z.; Liu, S.; Liu, R.; He, X.; Ma, J.; Xu, Z.; Zhou, J.; Wu, D. Simulating Oasis-Desert Interactions in Artificial and Natural Oasis-Desert Areas: Integration of Remote Sensing Data and CFD Methodology. *Agric. For. Meteorol.* **2025**, *367*, 110516. [CrossRef]
16. Zhi, X.; Anfuding, G.; Yang, G.; Gong, P.; Wang, C.; Li, Y.; Li, X.; Li, P.; Liu, C.; Qiao, C.; et al. Evaluation of the Water Resource Carrying Capacity on the North Slope of the Tianshan Mountains, Northwest China. *Sustainability* **2022**, *14*, 1905. [CrossRef]
17. Lai, J.; Li, Y.; Chen, J.; Niu, G.-Y.; Lin, P.; Li, Q.; Wang, L.; Han, J.; Luo, Z.; Sun, Y. Massive Crop Expansion Threatens Agriculture and Water Sustainability in Northwestern China. *Environ. Res. Lett.* **2022**, *17*, 034003. [CrossRef]
18. Song, Y.; Xue, D.; Ma, B.; Xia, S.; Ye, H. Farming in Arid Areas Depletes China's Water. *Science* **2023**, *379*, 651. [CrossRef]
19. Qi, X.; Feng, K.; Sun, L.; Zhao, D.; Huang, X.; Zhang, D.; Liu, Z.; Baiocchi, G. Rising Agricultural Water Scarcity in China Is Driven by Expansion of Irrigated Cropland in Water Scarce Regions. *One Earth* **2022**, *5*, 1139–1152. [CrossRef]
20. Xiang, W.; Tan, M.; Yang, X.; Li, X. The Impact of Cropland Spatial Shift on Irrigation Water Use in China. *Environ. Impact Assess. Rev.* **2022**, *97*, 106904. [CrossRef]
21. Wang, H.; Wang, Z.; Bai, Y.; Wan, W.; Wang, W.; Wang, K. Risk Assessment Method for Soil Secondary Salinization Based on Hydrological Frequency Analysis. *Ecol. Indic.* **2025**, *176*, 113688. [CrossRef]
22. Wang, J.; Ding, J.; Wang, Y.; Ge, X.; Lizaga, I.; Chen, X. Soil Salinization in Drylands: Measure, Monitor, and Manage. *Ecol. Indic.* **2025**, *175*, 113608. [CrossRef]
23. Zhao, Y.; Li, T.; Zhao, J.; Zhang, Z.; Liu, R.; Shi, Y.; Ma, H.; Zhao, C.; Liu, Z.; Yang, X. Rice Water Requirement Exacerbates Groundwater Depletion in Northeast China under a Changing Climate. *Agric. For. Meteorol.* **2025**, *371*, 110624. [CrossRef]
24. Li, W.; Kang, S.; Du, T.; Ding, R.; Zou, M. Optimal Groundwater Depth and Irrigation Amount Can Mitigate Secondary Salinization in Water-Saving Irrigated Areas in Arid Regions. *Agric. Water Manag.* **2024**, *302*, 109007. [CrossRef]
25. Wei, D.; Wang, X.; Luo, N.; Zhu, Y.; Wang, P.; Meng, Q. Alleviating Groundwater Depletion While Realizing Food Security for Sustainable Development. *J. Clean. Prod.* **2023**, *393*, 136351. [CrossRef]
26. Bhattarai, N.; Lobell, D.B.; Balwinder-Singh; Fishman, R.; Kustas, W.P.; Pokhrel, Y.; Jain, M. Warming Temperatures Exacerbate Groundwater Depletion Rates in India. *Sci. Adv.* **2023**, *9*, eadi1401. [CrossRef]
27. Feng, G.; Jin, W.; Ouyang, Y.; Huang, Y. The Role of Changing Land Use and Irrigation Scheduling in Groundwater Depletion Mitigation in a Humid Region. *Agric. Water Manag.* **2024**, *291*, 108606. [CrossRef]
28. Han, Y.; Jia, S. An Assessment of the Water Resources Carrying Capacity in Xinjiang. *Water* **2022**, *14*, 1510. [CrossRef]
29. Wang, J.; Zhang, F.; Jim, C.-Y.; Chan, N.W.; Johnson, V.C.; Liu, C.; Duan, P.; Bahtebay, J. Spatio-Temporal Variations and Drivers of Ecological Carrying Capacity in a Typical Mountain-Oasis-Desert Area, Xinjiang, China. *Ecol. Eng.* **2022**, *180*, 106672. [CrossRef]
30. Hao, L.; Su, X.; Singh, V.P.; Zhang, L.; Zhang, G. Suitable Oasis and Cultivated Land Scales in Arid Regions Based on Ecological Health. *Ecol. Indic.* **2019**, *102*, 33–42. [CrossRef]
31. Wu, X.; Zheng, Y.; Wu, B.; Tian, Y.; Zheng, C. Optimizing Conjunctive Use of Surface Water and Groundwater for Irrigation to Address Human-Nature Water Conflicts: A Surrogate Modeling Approach. *Agric. Water Manag.* **2016**, *163*, 380–392. [CrossRef]
32. Zou, C.; Chen, D.; Chang, Z.; Fan, J.; Zheng, J.; Zhao, H.; Wang, Z.; Li, H. Early Identification of Cotton Fields Based on Gf-6 Images in Arid and Semiarid Regions (China). *Remote Sens.* **2023**, *15*, 5326. [CrossRef]
33. Zhou, C.; Huang, J.; Xiao, Y.; Du, M.; Li, S. A Novel Approach: Coupling Prior Knowledge and Deep Learning Methods for Large-Scale Plastic Greenhouse Extraction Using Sentinel-1/2 Data. *Int. J. Appl. Earth Obs. Geoinf.* **2024**, *132*, 104073. [CrossRef]
34. Liang, J.; Sawut, M.; Cui, J.; Hu, X.; Xue, Z.; Zhao, M.; Zhang, X.; Rouzi, A.; Ye, X.; Xilike, A. Object-Oriented Multi-Scale Segmentation and Multi-Feature Fusion-Based Method for Identifying Typical Fruit Trees in Arid Regions Using Sentinel-1/2 Satellite Images. *Sci. Rep.* **2024**, *14*, 18230. [CrossRef]
35. Qi, H.; Qian, X.; Shang, S.; Wan, H. Multi-Year Mapping of Cropping Systems in Regions with Smallholder Farms from Sentinel-2 Images in Google Earth Engine. *GISci. Remote Sens.* **2024**, *61*, 2309843. [CrossRef]
36. Zhang, H.; Wang, Y.; Shang, J.; Liu, M.; Li, Q. Investigating the Impact of Classification Features and Classifiers on Crop Mapping Performance in Heterogeneous Agricultural Landscapes. *Int. J. Appl. Earth Obs. Geoinf.* **2021**, *102*, 102388. [CrossRef]
37. Sang, Z.; Liang, J.; Zheng, H.; Wang, K.; Xu, Y.; Liu, Y. Identification of Fragmented Cropland in Arid and Semiarid Sandy Areas: A Case Study of Horqin Left Rear Banner. *Front. Environ. Sci.* **2022**, *10*, 964403. [CrossRef]
38. Fernando, W.A.M.; Senanayake, I.P. Developing a Two-Decadal Time-Record of Rice Field Maps Using Landsat-Derived Multi-Index Image Collections with a Random Forest Classifier: A Google Earth Engine Based Approach. *Inf. Process. Agric.* **2024**, *11*, 260–275. [CrossRef]
39. Xie, Y.; Nhu, A.N.; Song, X.-P.; Jia, X.; Skakun, S.; Li, H.; Wang, Z. Accounting for Spatial Variability with Geo-Aware Random Forest: A Case Study for US Major Crop Mapping. *Remote Sens. Environ.* **2025**, *319*, 114585. [CrossRef]
40. Hu, X.; Xu, Y.; Huang, P.; Yuan, D.; Song, C.; Wang, Y.; Cui, Y.; Luo, Y. Identifying Changes and Their Drivers in Paddy Fields of Northeast China: Past and Future. *Agriculture* **2024**, *14*, 1956. [CrossRef]

41. Yu, L.; Xie, H.; Xu, Y.; Li, Q.; Jiang, Y.; Tao, H.; Aihemaiti, M. Identification and Monitoring of Irrigated Areas in Arid Areas Based on Sentinel-2 Time-Series Data and a Machine Learning Algorithm. *Agriculture* **2024**, *14*, 1693. [CrossRef]
42. Hou, Z.; Chen, B.; Liu, Y.; Zang, H.; Manevski, K.; Chen, F.; Yang, Y.; Ge, J.; Zeng, Z. High Resolution Crop Type and Rotation Mapping in Farming-Pastoral Ecotone in China Using Multi-Satellite Imagery and Google Earth Engine. *Remote Sens.* **2025**, *17*, 1707. [CrossRef]
43. Schmitt, R.J.P.; Rosa, L.; Daily, G.C. Global Expansion of Sustainable Irrigation Limited by Water Storage. *Proc. Natl. Acad. Sci. USA* **2022**, *119*, e2214291119. [CrossRef] [PubMed]
44. Mokhtari, S.; Benmehaia, A.M.; Nourani, A.; Hadjeb, A. Future Water Requirements of the Wheat Crop in Northern Algeria under Climate Change Scenarios. *Reg. Environ. Change* **2025**, *25*, 51. [CrossRef]
45. Fan, S.; Liu, T.; Zou, M.; Fang, Y.; Niu, J.; Kang, S. Spatiotemporal Dynamics and Driving Factors of Irrigation Water Demands in China. *Agric. Water Manag.* **2025**, *312*, 109450. [CrossRef]
46. Garcia-Lopez, S.; Salazar-Rojas, M.; Velez-Nicolas, M.; Isidoro, J.M.G.P.; Ruiz-Ortiz, V. Estimation of Evaporation in Andalusian Reservoirs: Proposal of an Index for the Assessment and Classification of Dams. *J. Hydrol. Reg. Stud.* **2025**, *58*, 102224. [CrossRef]
47. Zomer, R.J.; Xu, J.; Trabucco, A. Version 3 of the Global Aridity Index and Potential Evapotranspiration Database. *Sci. Data* **2022**, *9*, 409. [CrossRef]
48. Gonzalez, T.F.; Pavek, M.J.; Holden, Z.J.; Garza, R. Evaluating Potato Evapotranspiration and Crop Coefficients in the Columbia Basin of Washington State. *Agric. Water Manag.* **2023**, *286*, 108371. [CrossRef]
49. Bai, Y.; Xuan, X.; Wang, Y.; Weng, C.; Huang, X.; Deng, X. Revealing the Nexus Profile of Agricultural Water-Land-Food-GHG Flows in China. *Resour. Conserv. Recycl.* **2024**, *204*, 107528. [CrossRef]
50. Yan, Y.; Ryu, Y.; Li, B.; Dechant, B.; Zaheer, S.A.; Kang, M. A Multi-Objective Optimization Approach to Simultaneously Halve Water Consumption, CH_4, and N_2O Emissions While Maintaining Rice Yield. *Agric. For. Meteorol.* **2024**, *344*, 109785. [CrossRef]
51. Ma, S.; Ritsema, C.J.; Wang, S. Achieving Sustainable Crop Management: A Holistic Approach to Crop Competitiveness Assessment and Structure Optimization with Dual Natural-Social Environmental Impacts. *Agric. Syst.* **2024**, *218*, 103968. [CrossRef]
52. Wang, Y.; Wang, H.; Sun, J.; Qi, P.; Zhang, W.; Zhang, G. Spatially Optimized Allocation of Water and Land Resources Based on Multi-Dimensional Coupling of Water Quantity, Quality, Efficiency, Carbon, Food, and Ecology. *Agric. Water Manag.* **2025**, *309*, 109340. [CrossRef]
53. He, P.; Yu, S.; Ding, J.; Ma, T.; Li, J.; Dai, Y.; Chen, K.; Peng, S.; Zeng, G.; Guo, S. Multi-Objective Optimization of Farmland Water Level and Nitrogen Fertilization Management for Winter Wheat Cultivation under Waterlogging Conditions Based on TOPSIS-Entropy. *Agric. Water Manag.* **2024**, *297*, 108840. [CrossRef]
54. Su, Z.; Zhao, J.; Zhuang, M.; Liu, Z.; Zhao, C.; Pullens, J.W.M.; Liu, K.; Harrison, M.T.; Yang, X. Climate-Adaptive Crop Distribution Can Feed Food Demand, Improve Water Scarcity, and Reduce Greenhouse Gas Emissions. *Sci. Total Environ.* **2024**, *944*, 173819. [CrossRef]
55. Sun, J.; Yang, Y.; Qi, P.; Zhang, G.; Wu, Y. Development and Application of a New Water-Carbon-Economy Coupling Model (WCECM) for Optimal Allocation of Agricultural Water and Land Resources. *Agric. Water Manag.* **2024**, *291*, 108608. [CrossRef]
56. Wang, Y.; Shi, F.; Yao, P.; Sheng, Y.; Zhao, C. Assessing the Evolution and Attribution of Watershed Resilience in Arid Inland River Basins, Northwest China. *Sci. Total Environ.* **2024**, *906*, 167534. [CrossRef]
57. Qi, S.; Shu, H.; Feng, Q.; Zhu, M.; Liu, W.; He, J. Quantifying Recharge Sources to Groundwater to an Oasis Area: Implications for Strengthening Water Resource Management under Changing Environmental Conditions. *Hydrol. Process.* **2023**, *37*, 15049. [CrossRef]
58. Wei, J.; Dong, W.; Liu, S.; Song, L.; Zhou, J.; Xu, Z.; Wang, Z.; Xu, T.; He, X.; Sun, J. Mapping Super High Resolution Evapotranspiration in Oasis-Desert Areas Using UAV Multi-Sensor Data. *Agric. Water Manag.* **2023**, *287*, 108466. [CrossRef]
59. Miao, M.; Zhang, M.; Wang, S.; Sun, Z.; Li, X.; Yuan, X.; Yang, G.; Hu, Z.; Zhang, S. Effect of Oasis and Irrigation on Mountain Precipitation in the Northern Slope of Tianshan Mountains Based on Stable Isotopes. *J. Hydrol.* **2024**, *635*, 131151. [CrossRef]
60. Deng, H.; Pan, X.; Zhang, H.; Xiao, Z.; Xiao, R.; Zhao, Z.; Chen, T. Comprehensive Regulation of Water-Nitrogen Coupling in Hybrid Seed Maize in the Hexi Oasis Irrigation Area Based on the Synergy of Multiple Indicators. *Water* **2023**, *15*, 3927. [CrossRef]
61. Yang, P.; Zhu, Y.; Zhai, X.; Xia, J.; Chen, Y.; Huang, H.; Li, Z.; Shi, X.; Zhou, L.; Fu, C. Adaptive Management of Water Resources System in the Arid Aksu River Basin, Northwest China. *J. Clean. Prod.* **2023**, *419*, 138185. [CrossRef]
62. Fang, G.; Chen, Y.; Li, Z. Variation in Agricultural Water Demand and Its Attributions in the Arid Tarim River Basin. *J. Agric. Sci.* **2018**, *156*, 301–311. [CrossRef]
63. Farr, T.G.; Rosen, P.A.; Caro, E.; Crippen, R.; Duren, R.; Hensley, S.; Kobrick, M.; Paller, M.; Rodriguez, E.; Roth, L.; et al. The Shuttle Radar Topography Mission. *Rev. Geophys.* **2007**, *45*, RG2004. [CrossRef]
64. Pinkeaw, S.; Boonrat, P.; Koedsin, W.; Huete, A. Semi-Automated Mangrove Mapping at National-Scale Using Sentinel-2, Sentinel-1, and SRTM Data with Google Earth Engine: A Case Study in Thailand. *Egypt. J. Remote Sens. Space Sci.* **2024**, *27*, 555–564. [CrossRef]

65. Gao, Q.; Wu, T.; Tang, H.; Yang, J.; Wang, S. Large Area Crops Mapping by Phenological Horizon Attention Transformer (PHAT) Method Using MODIS Time-Series Imagery. *IEEE J. Sel. Top. Appl. Earth Obs. Remote Sens.* **2025**, *18*, 10995–11013. [CrossRef]
66. Newete, S.W.; Abutaleb, K.; Chirima, G.J.; Dabrowska-Zielinska, K.; Gurdak, R. Phenology-Based Winter Wheat Classification for Crop Growth Monitoring Using Multi-Temporal Sentinel-2 Satellite Data. *Egypt. J. Remote Sens. Space Sci.* **2024**, *27*, 695–704. [CrossRef]
67. Luo, J.; Xie, M.; Wu, Q.; Luo, J.; Gao, Q.; Shao, X.; Zhang, Y. Early Crop Identification Study Based on Sentinel-1/2 Images with Feature Optimization Strategy. *Agriculture* **2024**, *14*, 990. [CrossRef]
68. Liu, M.; Wang, J.; Fetisov, D.; Li, K.; Xu, C.; Jiang, J. Machine Learning-Based Fine Classification of Agricultural Crops in the Cross-Border Basin of the Heilongjiang River between China and Russia. *Remote Sens.* **2024**, *16*, 1670. [CrossRef]
69. Hao, P.-Y.; Tang, H.-J.; Chen, Z.-X.; Meng, Q.-Y.; Kang, Y.-P. Early-Season Crop Type Mapping Using 30-m Reference Time Series. *J. Integr. Agric.* **2020**, *19*, 1897–1911. [CrossRef]
70. Saenz, C.; Cicuendez, V.; Garcia, G.; Madruga, D.; Recuero, L.; Bermejo-Saiz, A.; Litago, J.; de la Calle, I.; Palacios-Orueta, A. New Insights on the Information Content of the Normalized Difference Vegetation Index Sentinel-2 Time Series for Assessing Vegetation Dynamics. *Remote Sens.* **2024**, *16*, 2980. [CrossRef]
71. Luo, W.; Chen, M.; Kang, Y.; Li, W.; Li, D.; Cui, Y.; Khan, S.; Luo, Y. Analysis of Crop Water Requirements and Irrigation Demands for Rice: Implications for Increasing Effective Rainfall. *Agric. Water Manag.* **2022**, *260*, 107285. [CrossRef]
72. Cao, X.; Wang, Y.; Wu, P.; Zhao, X.; Wang, J. An Evaluation of the Water Utilization and Grain Production of Irrigated and Rain-Fed Croplands in China. *Sci. Total Environ.* **2015**, *529*, 10–20. [CrossRef]
73. Miao, Q.; Rosa, R.D.; Shi, H.; Paredes, P.; Zhu, L.; Dai, J.; Goncalves, J.M.; Pereira, L.S. Modeling Water Use, Transpiration and Soil Evaporation of Spring Wheat-Maize and Spring Wheat-Sunflower Relay Intercropping Using the Dual Crop Coefficient Approach. *Agric. Water Manag.* **2016**, *165*, 211–229. [CrossRef]
74. Zhao, J.; Xu, J.; Ma, L.; Ma, Y. Effects of Different Irrigation Quotas on Water Consumption and Yield of Sunflower. *Agric. Res. Arid Areas* **2019**, *37*, 108–116.
75. Song, C.; Wang, Z.; Zheng, X.; Jiang, G.; Li, W.; Li, Z.; Chen, X. Determination of Water Consumption Characteristics and Crop Coefficient of Spring Wheat under Drip Irrigation Condition in Northern Xinjiang. *Acat Agric. Boreali-Occident. Sin.* **2013**, *22*, 58–63.
76. Yang, G.; Yu, W.; Yao, X.; Zheng, H.; Cao, Q.; Zhu, Y.; Cao, W.; Cheng, T. AGTOC: A Novel Approach to Winter Wheat Mapping by Automatic Generation of Training Samples and One-Class Classification on Google Earth Engine. *Int. J. Appl. Earth Obs. Geoinf.* **2021**, *102*, 102446. [CrossRef]
77. Gong, P.; Liu, H.; Zhang, M.; Li, C.; Wang, J.; Huang, H.; Clinton, N.; Ji, L.; Li, W.; Bai, Y. Stable Classification with Limited Sample: Transferring a 30-m Resolution Sample Set Collected in 2015 to Mapping 10-m Resolution Global Land Cover in 2017. *Sci. Bull.* **2019**, *64*, 370–373. [CrossRef]
78. Zhang, X.; Liu, L.; Chen, X.; Gao, Y.; Xie, S.; Mi, J. GLC_FCS30: Global Land-Cover Product with Fine Classification System at 30 m Using Time-Series Landsat Imagery. *Earth Syst. Sci. Data Discuss.* **2020**, *13*, 2753–2776. [CrossRef]
79. You, N.; Dong, J.; Huang, J.; Du, G.; Xiao, X. The 10-m Crop Type Maps in Northeast China during 2017–2019. *Sci. Data* **2021**, *8*, 41. [CrossRef]
80. Xu, J.; Liu, X.; Yang, S.; Qi, Z.; Wang, Y. Modeling Rice Evapotranspiration under Water-Saving Irrigation by Calibrating Canopy Resistance Model Parameters in the Penman-Monteith Equation. *Agric. Water Manag.* **2017**, *182*, 55–66. [CrossRef]
81. Li, F.; Ma, Y. Evaluation of the Dual Crop Coefficient Approach in Estimating Evapotranspiration of Drip-Irrigated Summer Maize in Xinjiang, China. *Water* **2019**, *11*, 1053. [CrossRef]
82. Sezen, S.M.; Yazar, A.; Kapur, B.; Tekin, S. Comparison of Drip and Sprinkler Irrigation Strategies on Sunflower Seed and Oil Yield and Quality under Mediterranean Climatic Conditions. *Agric. Water Manag.* **2011**, *98*, 1153–1161. [CrossRef]
83. Xiao, Y.; Zhang, J.; Jia, T.T.; Pang, X.P.; Guo, Z.G. Effects of Alternate Furrow Irrigation on the Biomass and Quality of Alfalfa (*Medicago sativa*). *Agric. Water Manag.* **2015**, *161*, 147–154. [CrossRef]
84. French, A.N.; Hunsaker, D.J.; Bounoua, L.; Karnieli, A.; Luckett, W.E.; Strand, R. Remote Sensing of Evapotranspiration over the Central Arizona Irrigation and Drainage District, USA. *Agronomy* **2018**, *8*, 278. [CrossRef]
85. Howell, T.A.; Evett, S.R.; Tolk, J.A.; Copeland, K.S.; Marek, T.H. Evapotranspiration, Water Productivity and Crop Coefficients for Irrigated Sunflower in the US Southern High Plains. *Agric. Water Manag.* **2015**, *162*, 33–46. [CrossRef]
86. Wang, Y.; Zhao, J. Temporal-Spatial Patterns of the Water Deficit in the Main Maize-Cropping Regions of China. *Agronomy* **2025**, *15*, 728. [CrossRef]
87. Feng, Y.; Guo, Y.; Shen, Y.; Zhang, G.; Wang, Y.; Chen, X. Change of Crop Structure Intensified Water Supply-Demand Imbalance in China's Black Soil Granary. *Agric. Water Manag.* **2024**, *306*, 109199. [CrossRef]
88. Kropp, I.; Nejadhashemi, A.P.; Deb, K.; Abouali, M.; Roy, P.C.; Adhikari, U.; Hoogenboom, G. A Multi-Objective Approach to Water and Nutrient Efficiency for Sustainable Agricultural Intensification. *Agric. Syst.* **2019**, *173*, 289–302. [CrossRef]

89. Zhang, J.; Zhao, L.; Yang, H. A Dual-Branch U-Net for Staple Crop Classification in Complex Scenes. *Remote Sens.* **2025**, *17*, 726. [CrossRef]
90. He, Y.; Dong, J.; Liao, X.; Sun, L.; Fu, P. Examining Rice Distribution and Cropping Intensity in a Mixed Single- and Double-Cropping Region in South China Using All Available Sentinel 1/2 Images. *Int. J. Appl. Earth Obs. Geoinf.* **2021**, *101*, 102351. [CrossRef]
91. Yuan, Q.; Shen, H.; Li, T.; Li, Z.; Li, S.; Jiang, Y.; Xu, H.; Tan, W.; Yang, Q.; Wang, J.; et al. Deep Learning in Environmental Remote Sensing: Achievements and Challenges. *Remote Sens. Environ.* **2020**, *241*, 111716. [CrossRef]
92. Rehman, A.U.; Raziq, A.; Shrestha, B.; Nguyen, K.-A.; Liou, Y.-A. The Role of Spectro-Temporal Remote Sensing in Vegetation Classification: A Comprehensive Review Integrating Machine Learning and Bibliometric Analysis. *Comput. Electron. Agric.* **2025**, *234*, 110184. [CrossRef]
93. Li, G.; Han, W.; Wei, J.; Shang, M.; Xiong, D.; Zhai, X.; Huang, S.; Zhang, L. The Suitable Spatial Resolution of Crop Type Mapping at Plot-Level in Hetao Irrigation District of China Based on UAV Remote Sensing. *Int. J. Remote Sens.* **2025**, *46*, 4654–4678. [CrossRef]
94. Li, Z.; Xiao, Z.; Zhou, Y.; Bao, T. Typical Crop Classification of Agricultural Multispectral Remote Sensing Images by Fusing Multi-Attention Mechanism ResNet Networks. *Sensors* **2025**, *25*, 2237. [CrossRef]
95. Kim, H.-J.; Chandrasekara, S.; Kwon, H.-H.; Lima, C.; Kim, T. A Novel Multi-Scale Parameter Estimation Approach to the Hargreaves-Samani Equation for Estimation of Penman-Monteith Reference Evapotranspiration. *Agric. Water Manag.* **2023**, *275*, 108038. [CrossRef]
96. Tan, Q.; Liu, Y.; Pan, T.; Song, X.; Li, X. Changes and Determining Factors of Crop Evapotranspiration Derived from Satellite-Based Dual Crop Coefficients in North China Plain. *Crop J.* **2022**, *10*, 1496–1506. [CrossRef]
97. Al Tamimi, M.; Green, S.; Hammami, Z.; Ammar, K.; Al Ketbi, M.; Al-Shrouf, A.M.; Dawoud, M.; Kennedy, L.; Clothier, B. Evapotranspiration and Crop Coefficients Using Lysimeter Measurements for Food Crops in the Hyper-Arid United Arab Emirates. *Agric. Water Manag.* **2022**, *272*, 107826. [CrossRef]
98. Liu, J.; Sun, B.; Shen, H.; Ding, P.; Ning, D.; Zhang, J.; Qiu, X. Crop Water Requirement and Utilization Efficiency-Based Planting Structure Optimization in the Southern Huang-Huai-Hai Plain. *Agronomy* **2022**, *12*, 2219. [CrossRef]
99. Tian, Y.; Liu, W.; Chen, T.; Chen, S.; Shi, H.; Chen, H. Variations in Wheat Water Requirement and Climatic Causes in Arid Regions of Northwest China. *Environ. Monit. Assess.* **2025**, *197*, 172. [CrossRef]
100. Gao, X.; Tang, P.; Wang, Z.; Yao, Y.; Qu, Z.; Yang, W.; Du, B. Crop Coefficient of Sunflowers under Drip Irrigation with Plastic Film in Different Hydrological Years in the Hetao Irrigation District. *Water* **2024**, *16*, 235. [CrossRef]
101. Djaman, K.; Koudahe, K.; Mohammed, A.T. Dynamics of Crop Evapotranspiration of Four Major Crops on a Large Commercial Farm: Case of the Navajo Agricultural Products Industry, New Mexico, USA. *Agronomy* **2022**, *12*, 2629. [CrossRef]
102. Zhao, N.; Zheng, X.; Zhang, B.; Tian, S.; Du, L.; Li, Y. Does Water-Saving Irrigation Truly Conserve Water? Yes and No. *Agric. Water Manag.* **2025**, *311*, 109399. [CrossRef]
103. Armengot, L.; Barbieri, P.; Andres, C.; Milz, J.; Schneider, M. Cacao Agroforestry Systems Have Higher Return on Labor Compared to Full-Sun Monocultures. *Agron. Sustain. Dev.* **2016**, *36*, 70. [CrossRef]
104. Shaver, I.; Chain-Guadarrama, A.; Cleary, K.A.; Sanfiorenzo, A.; Santiago-Garcia, R.J.; Finegan, B.; Hormel, L.; Sibelet, N.; Vierling, L.A.; Bosque-Perez, N.A.; et al. Coupled Social and Ecological Outcomes of Agricultural Intensification in Costa Rica and the Future of Biodiversity Conservation in Tropical Agricultural Regions. *Glob. Environ. Change-Hum. Policy Dimens.* **2015**, *32*, 74–86. [CrossRef]
105. Lago-Olveira, S.; Rebolledo-Leiva, R.; Garofalo, P.; Moreira, M.T.; Gonzalez-Garcia, S. Environmental and Economic Benefits of Wheat and Chickpea Crop Rotation in the Mediterranean Region of Apulia (Italy). *Sci. Total Environ.* **2023**, *896*, 165124. [CrossRef]
106. Misiewicz, A.; Mikolajczyk, L.; Bednarska, A.J. Impact of Oilseed Rape Coverage and Other Agricultural Landscape Characteristics on Two Generations of the Red Mason Bee Osmia Bicornis. *Agric. Ecosyst. Environ.* **2023**, *352*, 108514. [CrossRef]
107. Gu, B.; Xu, L.; Fu, Y.; Chen, J. Green Agricultural Technology Extension Strategies Considering Industrial Organization Impacts: Direct Subsidy VS Indirect Incentive. *J. Clean. Prod.* **2024**, *479*, 143991. [CrossRef]
108. Parra-Lopez, C.; Abdallah, S.B.; Garcia-Garcia, G.; Hassoun, A.; Sanchez-Zamora, P.; Trollman, H.; Jagtap, S.; Carmona-Torres, C. Integrating Digital Technologies in Agriculture for Climate Change Adaptation and Mitigation: State of the Art and Future Perspectives. *Comput. Electron. Agric.* **2024**, *226*, 109412. [CrossRef]
109. Parra-Lopez, C.; Ben Abdallah, S.; Garcia-Garcia, G.; Hassoun, A.; Trollman, H.; Jagtap, S.; Gupta, S.; Ait-Kaddour, A.; Makmuang, S.; Carmona-Torres, C. Digital Technologies for Water Use and Management in Agriculture: Recent Applications and Future Outlook. *Agric. Water Manag.* **2025**, *309*, 109347. [CrossRef]
110. Lun, R.; Liu, W.; Li, G.; Luo, Q. Does Digital Agricultural Technology Extension Service Enhance Sustainable Food Production? Evidence from Maize Farmers in China. *Agriculture* **2024**, *14*, 292. [CrossRef]

111. Chen, Y.; Xiang, W.; Zhao, M. Impacts of Capital Endowment on Farmers' Choices in Fertilizer-Reduction and Efficiency-Increasing Technologies (Preferences, Influences, and Mechanisms): A Case Study of Apple Farmers in the Provinces of Shaanxi and Gansu, China. *Agriculture* **2024**, *14*, 147. [CrossRef]
112. Xu, B.; Liu, W. The Real Impact of Digital Agricultural Technology Extension on Pesticide Reduction Behavior among Wheat Farmers in Henan, China. *Agriculture* **2025**, *15*, 1002. [CrossRef]
113. Ostrom, E. A General Framework for Analyzing Sustainability of Social-Ecological Systems. *Science* **2009**, *325*, 419–422. [CrossRef] [PubMed]
114. Zhang, J.; Wang, M.; Liu, K.; Chen, S.; Zhao, Z. Social-Ecological System Sustainability in China from the Perspective of Supply-Demand Balance for Ecosystem Services. *J. Clean. Prod.* **2025**, *497*, 145039. [CrossRef]

Disclaimer/Publisher's Note: The statements, opinions and data contained in all publications are solely those of the individual author(s) and contributor(s) and not of MDPI and/or the editor(s). MDPI and/or the editor(s) disclaim responsibility for any injury to people or property resulting from any ideas, methods, instructions or products referred to in the content.